NASA TT F-11,320

PROBLEMS OF EVALUATION OF DIFFERENTIAL ANGULAR CORRELATION MEASUREMENTS WITH A FOUR-DETECTOR APPARATUS AND INVESTIGATIONS WITH Yb-172

H.F.Wagner

FACILITY FORM 602

N 68-26177 (ACCESSION NUMBER)

43 (PAGES)

CR-94936 (NASA CR OR TMX OR AD NUMBER)

1 (THRU)

(CODE)

24 (CATEGORY)

Translation of "Auswerteprobleme bei einer Vier-Detektor-Apparatur zur differentiellen Messung von Winkelkorrelationen und Messungen am Yb 172". Report BMwF-FB K66-39, Bundesministerium für wissenschaftliche Forschung, Bonn, July 1966.

GPO PRICE $ _____

CFSTI PRICE(S) $ _____

Hard copy (HC) 3.00

Microfiche (MF) _____

ff 653 July 65

JUN 1968 RECEIVED NASA STI FACILITY INPUT BRANCH

NATIONAL AERONAUTICS AND SPACE ADMINISTRATION
WASHINGTON, D.C. 20546 JUNE 1968

TABLE OF CONTENTS

PRECEDING PAGE BLANK NOT FILMED

PROBLEMS OF EVALUATION OF DIFFERENTIAL ANGULAR CORRELATION MEASUREMENTS WITH A FOUR-DETECTOR APPARATUS AND INVESTIGATIONS WITH Yb-172

/1*

H.F.Wagner

ABSTRACT. Formulas for differential angular correlation measurements are derived and discussed. The formulas are applied to the problem of a four-detector apparatus, using a digital computer program. The fully transistorized automatic control of the apparatus is described in detail, with discussion of differential measurements of the 203 - 1095 Kev cascade of Yb^{172}. As result, $A_2(0) = -0.065 \pm 0.021$; $A_4(0) = +0.003 \pm 0.025$ are given, with $T_{1/2} = (8.34 \pm 0.20)$ ns for the 1174 Kev level.

I. INTRODUCTION

One of the most important methods for obtaining information on the data of excited nuclear levels consists in an investigation of gamma-gamma angular correlations. For this, two experimental methods are available: the integral and the differential coincidence measuring technique.

Of these two procedures, the differential method permits a time resolution of the angular correlation and thus furnishes a possibility of measuring the differential attenuation factors λ_k. Their accurate determination is of great theoretical interest since, on their basis and with the aid of the theory of perturbed gamma-gamma angular correlations, it becomes possible to obtain statements on fields existing at the nuclear site and, in favorable cases, to calculate the moments of excited nuclear levels.

For an accurate measurement of these parameters λ_k, our study group constructed an apparatus, working with four detectors and four coincidence circuits. This arrangement, compared to setups with two detectors, reduces the statistical error of the test data by a factor of 2.

The present paper gives a description of the various parts of this four-detector apparatus and discusses the processing of the resultant data. Other parts of the instrument are described in the thesis by K.Krien (Ref.12).

The discussion of the data processing is subdivided into two parts: In the first part, all formulas describing the time course of differentially measured angular correlation coefficients are systematically derived and discussed. This is done in Section 2 of this paper. In the second part, the computer programs

* Numbers in the margin indicate pagination in the foregin text.

required for data processing are described, with main emphasis on an expansion and matching program based on the formulas introduced in the first part. This will be discussed in Section 4.

In Section 5, a differential angular correlation measurement with the four-detector instrument on the 203 - 1095 Kev cascade of ytterbium-172 will be re- /2
ported, whose interpretation is based on the introduced formulas and the described computer program.

II. INTRODUCTION OF THE MOST IMPORTANT EQUATIONS FOR DIFFERENTIAL COINCIDENCE MEASUREMENTS /3

1. Perturbed and Unperturbed Gamma-Gamma Angular Correlations and their Measuring Techniques

By the concept of gamma-gamma angular correlation we mean the following phenomenon: If a nucleus gives off its excitation energy under emission of two successive gamma quanta, the two emission directions will be correlated under certain assumptions. This means that the angle ϑ between the two emission directions can occur only with a probability $W(\vartheta)$ which depends on the spin of the participating levels and on the multipolarities of the two gamma transitions. One generally differentiates between unperturbed and perturbed angular correlations, of which each requires a different measuring method, either the integral or the differential coincidence technique.

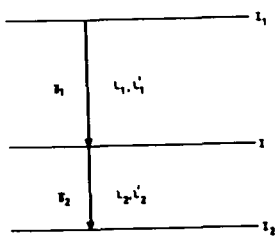

Fig.1 Scheme of a Gamma Cascade.

Unperturbed angular correlations are observed in nuclei which, in the intermediate state, do not interact with external fields. In this case, the magnetic sublevels of the intermediate state are degenerate and the nucleus retains its spatial orientation. In that case, the theory (Ref.1) shows that $W(\vartheta)$ can be expressed by an expansion in Legendre polynomials of the following form:

$$W(\vartheta) = 1 + \sum_{K=2}^{K_{max}} A_K P_K(\cos\vartheta), \text{ mit } K_{max} = \text{Min}(2L_1', 2L_2', 2I)$$

A perturbation of the angular correlation apparently occurs whenever fields exist at the nuclear site with which the nuclear moments are able to interact. /4
This will cancel the degeneration of the intermediate level and the nucleus becomes able to change its orientation by transitions between the sublevels. The degree of the resultant perturbation will be dependent on duration, intensity, and nature of the interaction.

These three parameters, at perturbed angular correlation, must be contained

in the expression for the probability distribution of the angle ϑ. If τ denotes the duration of the interaction and if the parameter s expresses its type and intensity, then $W(\vartheta)$ must change over into $W(\vartheta, \tau, s)$. For this expression, it is generally no longer possible to derive a simple expansion in Legendre polynomials.

Application of the integral measuring method in the presence of perturbations is useful only if these perturbations are so small that, in good approximation, $W(\vartheta)$ can be written for $W(\vartheta, \tau, s)$. This will be possible at weak interactions and short lifetimes. At strong interactions and long lifetimes, this approximation is no longer permissible so that the method of differential coincidence technique must be used, which permits a measurement of the angular correlation as a function of the interaction time τ. Here, τ is determined by the delay time interval existing between the two gamma quanta because of the finite lifetime of the intermediate level.

Such a differential measurement is of great interest for the theory of perturbed angular correlations. The method permits statements as to the perturbation fields at the nuclear site and as to properties of the nuclei in excited states, including magnetic moments and quadrupole moments. In addition, integrally measured angular correlations can be corrected for perturbations after a differential measurement. This is of decisive importance since an exact spin determination, on the basis of an integral measurement, is possible only after a correction for perturbation.

2. Differential Measuring Method

The principle of any experimental determination of angular correlations consists in measuring the coincidence counting rates between two detectors, at different angles. Here, the difference between the integral and differential /5
methods is the following: In the integral method, the coincidences are summed up over all delays τ. The coincidence counting rate is measured only under different angles. Conversely, in the differential technique, the coincidence counting rate is additionally observed as a function of the delay time τ between the two gamma quanta.

For this coincidence counting rate $N(\vartheta, \tau)$, an explicit expression is obtained from the following considerations: Because of the law of radioactive decay, the delay times are distributed in accordance with a function $g(\tau) = \lambda \cdot \exp(-\lambda\tau)$, where λ denotes the decay constant of the intermediate level. Since the coincidence arrangement has a finite time resolution $\Delta\tau$, the delay time τ cannot be defined exactly and only the interval from τ to $\tau + \Delta\tau$ is covered. The probability of recording a coincidence in this interval, at an angle ϑ, is given by the expression $g(\tau) \cdot \Delta\tau \cdot W(\vartheta, \tau, s)$. If N_0 allows for the detection probability and the activity, then the following expression is obtained for the number of coincidences at an angle ϑ and the delay time τ between the gamma quanta:

$$N(\vartheta,\tau) = N_0 \cdot \lambda \cdot e^{-\lambda\tau} \cdot W(\vartheta,\tau,s) \cdot \Delta\tau$$

To permit as accurate as possible a measurement of $N(\vartheta, \tau)$, the requirement that

$\Delta\tau \leq 1/\lambda$ must be made on the time resolution of the coincidence stage. Obviously, an accurate determination of the time differences is no longer possible for the case $\Delta\tau \gg 1/\lambda$, and the differential method passes over into the integral method.

Ever since the development of multichannel analyzers, a simple method for measuring $N(\vartheta, \tau)$ has been the use of time-pulse height converters. Such a converter represents a coincidence stage in which the height of the output pulse is proportional to the time spacing of the input signals. The individual operating principles of such converters have been discussed by M.Forker (Ref.2).

In the following Section we will discuss the slope of the function $N(\vartheta, \tau)$ when using the four-detector instrument described in Chapter III. /6

After briefly outlining the measuring principle, the time resolution properties of the apparatus are discussed since, as will be demonstrated, these properties enter $N(\vartheta, \tau)$ in a determinantal manner. This discussion leads to the concept of the "prompt curve" which is characteristic for the time resolution of the coincidence arrangement used. The influence of this prompt curve on the differentially measured coincidence counting rate will be discussed next. The result of this study yields an explicit expression for $N(\vartheta, \tau)$, mathematically consisting in a convolution integral whose kernel is formed by the prompt curve mirrored at the zero point.

3. Time Course of the Coincidence Counting Rate $N(\vartheta, \tau)$

a) Fast-Slow Principle

The four-detector instrument for differential measurement of gamma-gamma angular corrections operates on the fast-slow principle which had been described repeatedly in great detail (Ref.2, 4, 5). Here, the fast coincidence circuit is used for measuring the counting rate $N(\vartheta, \tau)$ and is built up as follows: Two NaI(Ta) scintillation crystals, with attached multipliers, serve as detectors that feed their signals, across pulse-shaping stages, to a coincidence loop. The latter is based on the converter principle, taken from a suggestion by P.C. Simms (Ref.6). The output signals of the converter are analyzed as to their pulse heights by means of a multichannel analyzer.

b) Prompt Curve

For determining the time resolution properties of this coincidence arrangement, let us define the permissible difference between two delays τ_1 and τ_2 at which two still separable pulse heights at the converter output can be observed. These two delays are experimentally realized by means of the 511-Kev positron annihilation radiation, in which the time difference of the two gamma quanta is exactly zero. The delays τ_1 and τ_2 can then be accurately adjusted by means /7 of cables.

On the basis of its operating principle of converting delay time intervals between the input signals into pulse heights, the converter should furnish two

different pulse heights in this experiment. However, an analysis with the multichannel analyzer, instead of the expected two δ-functions, yields two pulse height distributions which are mutually displaced in position within the channel. The course of the distributions is equal and exhibits a Gaussian distribution curve which, on both flanks, passes over into an e-function. The two delay times τ_1 and τ_2 are coordinated with the maxima of the two distributions. The remaining delay times t, which additionally occur in the distribution, are mainly produced by the two detectors. Experiments have shown (Ref.2) that the detectors superpose statistically constant delays to the given time intervals, which are of the order of magnitude of one nanosecond (Ref.3). In addition, it can be demonstrated that one edge each of the distribution is formed by the properties of one detector (Ref.2).

As demonstrated by the form of this pulse height distribution, known also as prompt curve, the time interval between τ_1 and τ_2 can be shorter the more narrow the distribution and the steeper its edges. For this reason, the half-width of the prompt curve is used in this coincidence arrangement for defining the time resolution.

Mathematically, the prompt curve should be described by a function $V(t, \tau_j)$ which, in the argument, contains the given delay τ_j as well as the remaining delay times t occurring in the distribution. As shown by experiment, τ_j determines only the position of the prompt curve but not its general slope. For this reason, $V(t, \tau_j)$ will be represented in a coordinate system in which the position of the prompt curve is independent of the parameter τ_j and in which the maximum is located at the origin. Such a system is obtained when selecting the connectivity $T - t - \tau_j$ for t and τ_j. Then, the expression $V(T) = V(t - \tau_j)$ is obtained for the prompt curve.

c) Influence of the Prompt Curve on $N(\vartheta, \tau)$ /8

Determination of the coincidence counting rate $N(\vartheta, \tau)$, in the coincidence arrangement described here, proceeds as follows: All coincidences that produce the same pulse height I at the converter output are added. This pulse height, on the basis of the prompt curve, can be produced by any delay between the gamma quanta. In this case, the probability of causing a pulse height I is different for each individual delay.

For a quantitative determination of these probabilities, an arbitrary delay τ_j between the quanta will be considered. This delay produces a prompt curve of the form $V(t - \tau_j)$ and, during disintegration of the nucleus, occurs with the probability $\lambda \cdot \exp(-\lambda\tau_j) \cdot W(\vartheta, \tau_j, s)$ if coincidences at an angle ϑ are observed. Then, τ_j will appear at the converter output and the pulse height I_j produced by τ_j will appear with the probability $\lambda \cdot \exp(-\lambda\tau_j) \cdot W(\vartheta, \tau_j, s) \cdot V(\tau_j - t)$. Any other delay $t \neq \tau_j$ between the quanta also produces a prompt curve in which τ_j and thus also I_j are present with the probability $V(\tau_j - t)$. This means that, in observations of coincidences at an angle ϑ, any delay t between the quanta will produce the pulse height I_j with the probability $\lambda \cdot \exp(-\lambda t) \cdot W(\vartheta, t, s) \cdot V(\tau_j - t)$. The total probability for the occurrence of I_j is then given by the sum of the individual probabilities for each t:

$$P(\vartheta,\tau_j) = \int_0^\infty \lambda \exp(-\lambda t)\cdot W(\vartheta,t,s)\cdot V(\tau_j - t)\cdot dt \ ,$$

where the integration starts with zero since, for times t shorter than zero, the expression loses all physical meaning. If N_0 is to allow for the detection probability of the quanta and the activity, then the coincidence counting rate, for each delay τ_j between the gamma quanta, is given by $N(\vartheta, \tau_j) = N_0 \cdot P(\vartheta, \tau_j)$. Since the prompt curve in these considerations enters all expressions as probability, it is necessary to norm its area to 1. For this reason, $N(\vartheta, \tau_j)$ must be divided by the norming integral. /9

$$I = \int_{-\infty}^{\infty} V(\tau_j - t)\, dt = \int_{-\infty}^{\infty} \varepsilon(t-\tau_j)\, dt$$

so that, as the final expression, we obtain

$$N(\vartheta,\tau_j) = (N_0/I)\cdot \int_0^\infty \exp(-\lambda t)\cdot W(\vartheta,t,s)\cdot \varepsilon(t-\tau_j)\, dt \qquad (1)$$

with $N_0\lambda \rightarrow N_0$. Because of $T = t - \tau_j$ and $V(-T) = \varepsilon(T)$ with $\varepsilon(t - \tau_j)$ the prompt curve mirrored at the point T = 0 was entered.

To calculate the slope of the function $N(\vartheta, \tau_j)$, explicit expressions must be derived for $\varepsilon(T)$ and $W(\vartheta, t, s)$, which will be done in the following Sections.

4. Analytical Representation of the Prompt Curve

One of the first arguments for an analytic representation of V(T) was derived by Hrynkievicz (Ref.7) and by Matthias et al. (Ref.8) who assumed a simple rectangular distribution for the function V(T). Because of the very rough approximation, this assumption furnished only qualitative statements. Another argument (Ref.9) used a Gaussian distribution $V(T) = \exp(-\pi(T/2T_R))$ where T_R gives the resolution time of the coincidence circuit (Ref.2). This argument again does not sufficiently consider the slope of the prompt curve in so far as the curve does have the form of a Gaussian curve in the neighborhood of the maximum but distinctly changes into a pure e-function along the flanks.

Since each flank is determined by the properties of one detector (Ref.2), the two decay constants λ_1 and λ_2 need not be equal, so that the prompt curve may have an entirely asymmetric slope. In that case, the half-width will also be asymmetrically distributed over the two halves of the curve, which makes it logical to introduce a 1/e width σ_1 for the right-hand side and of a 1/e width σ_2 for the left-hand side. For this reason, any argument for facilitating the /10

mathematical representation of the prompt curve should contain the parameters λ_1, λ_2, σ_1, σ_2 for fitting to the measured prompt curve. According to a sug-testion by C.Günther (Ref.10), we subdivided the prompt curve into four segments (Fig.2): starting at the left, an e-function with the decay constant λ_2, followed by a Gaussian curve with the 1/e width σ_2 up to the maximum, changing after the maximum into another Gaussian curve with σ_1 as 1/e width, and then returning again to an e-function which has λ_1 as decay constant.

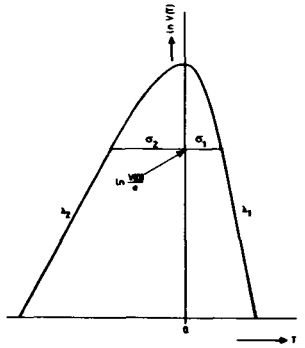

Fig.2 Slope of the Prompt Curve.

The mathematical argument then will read as follows:

$$V(T) = \begin{cases} B \cdot e^{\lambda_2 T} & -\infty \leq T \leq T_1 \\ e^{-\left(\frac{T}{\sigma_2}\right)^2} & T_1 \leq T \leq 0 \\ e^{-\left(\frac{T}{\sigma_1}\right)^2} & 0 \leq T \leq T_2 \\ B \cdot e^{-\lambda_1 T} & T_2 \leq T \leq \infty \end{cases}$$

Here, V(0) was arbitrarily normed to 1. The stipulation that the four subsegments should adjoin in a continuously differentiable manner results in two conditions for T_1 and A as well as for T_2 and B at the contact points T_1 and T_2, from which four equations are obtained which yield the following final expression for the prompt curve:

/11

$$V(T) = \begin{cases} e^{\lambda_2 \left(T + \frac{\sigma_2^2 \lambda_2}{2}\right)} & -\infty < T \leq -\frac{\sigma_2^2 \lambda_2}{2} \\ e^{-\left(\frac{T}{\sigma_2}\right)^2} & -\frac{\sigma_2^2 \lambda_2}{2} \leq T \leq 0 \\ e^{-\left(\frac{T}{\sigma_1}\right)^2} & 0 \leq T \leq \frac{\sigma_1^2 \lambda_1}{2} \\ e^{-\lambda_1 \left(T - \frac{\sigma_1^2 \lambda_1}{2}\right)} & \frac{\sigma_1^2 \lambda_1}{2} \leq T \leq \infty \end{cases}$$

Since thus also $\epsilon(T)$, as a function reflected at the origin, is known the following expression is obtained for the norming integral $I = \int_{-\infty}^{\infty} \epsilon(T)dt$:

$$I = \frac{1}{\lambda_1} e^{\frac{\lambda_1 T_1}{4}} + \frac{1}{\lambda_2} e^{\frac{\lambda_2 T_2}{4}} + \frac{\sqrt{\pi}}{2}\left[\sigma_1 \phi\left(-\frac{T_1}{\sigma_1}\right) + \sigma_2 \phi\left(\frac{T_2}{\sigma_2}\right)\right]$$

where the terms $\phi(x)$ represent abbreviations for the Gaussian probability integral.

5. Analytical Expression for the Probability $W(\vartheta, t, s)$

The explicit expression for $W(\vartheta, t, s)$ depends on the type of the perturbing interaction which may be dependent or independent of time.

A typical example for a time-independent perturbation is furnished by the spin rotation method. In this method, the angular correlation is influenced by a static magnetic field which is perpendicular to the plane of the detectors. In this case, the theory furnishes the following expression for $W(\vartheta, t, s)$:

$$W(\vartheta, t, s) = 1 + \sum_{k=2}^{K_{max}} A_k \cdot P_k(\cos(\vartheta - \omega t)) \quad , \quad K_{max} = \mathrm{Min}(2I, 2L_1', 2L_2')$$

One speaks of time-dependent perturbations whenever the fields change their direction at the nuclear site over intervals that are small with respect to $1/\lambda$. For example, this case exists in liquids when $1/\lambda \approx 10^{-9}$ sec, since the time for a change in direction of the perturbation fields has a magnitude of 10^{-11} to 10^{-13} sec. A theoretical study by A.Abragam and R.V.Pound (Ref.19) demonstrated that these perturbations cannot be averaged out but may actually lead to a strong attenuation of the angular correlation. Abragam and Pound, in deriving an expression for $W(\vartheta, t, s)$, used the method of the time-dependent perturbation theory and obtained /12

$$W(\vartheta, t, s) = 1 + \sum_{K=2,\ldots,K_{max}} A_K(\tau_j) \cdot P_k(\cos\vartheta) \quad K_{max} = \mathrm{Min}(2I, 2L_1', 2L_2')$$

with $A_k(\tau_j) = A_k(0) \exp(-\lambda_k \tau_j)$.

This leads to an expansion in Legendre polynomials, as it is possible also in the unperturbed case. In the perturbed case, the correlation coefficients are now time-variant and tend to zero with τ_j, which leads to an attenuation of the angular distribution. For this reason, the parameters λ_k are known as attenuation factors. These depend on the type of perturbation present, i.e., whether electric or magnetic interactions are involved, and permit - in favorable cases - a calculation of the magnetic moment or of the quadrupole moment of nuclei in excited states (Ref.10, 13).

In the subsequent calculations, the expression by Abragam and Pound is used for $W(\vartheta, t, s)$, since the four-detector instrument described in Chapter III was

built for an accurate measurement of the attenuation factors λ_k. On substituting this expression into eq.(1) of p.6, we obtain

$$N(\vartheta,\tau_j) = \frac{N_0}{I}\int_0^\infty \varepsilon(t-\tau_j)e^{-\lambda t}\left(1+\sum_K A_K(0)\cdot e^{-\lambda_K t}\cdot P_K(\cos\vartheta)\right)dt$$

$$= \frac{N_0}{I}\int_0^\infty \varepsilon(t-\tau_j)e^{-\lambda t}dt + \sum_K\left(\frac{N_0}{I}A_K(0)\int_0^\infty \varepsilon(t-\tau_j)\cdot e^{-(\lambda+\lambda_K)t}dt\right)P_K(\cos\vartheta)$$

$$= a_0(\tau_j) + \sum_K a_K(\tau_j)\cdot P_K(\cos\vartheta)$$

$$\frac{N(\vartheta,\tau_j)}{a_0(\tau_j)} = 1 + \sum_K A_K(\tau_j)\cdot P_K(\cos\vartheta)$$

On the basis of these formulas it is possible to calculate the coefficients /13
$A_k(\tau_j)$ and thus also the angular correlation as a function of the delay time τ_j of the gamma quanta, provided that the coincidence counting rate $N(\vartheta, \tau_j)$ is measured on three different angles. The procedure for calculating these coefficients from the coincidence counting rates had been described at various occasions (Ref.12).

In the following Sections, the time course of the individual coefficients will be discussed in more detail.

6. Course of the Coefficient $a_0(\tau_j)$

The time variance of the coefficient $a_0(\tau_j)$ is given by the following equation:

$$a_0(\tau_j) = N_0\cdot e^{-\lambda\tau_j}\cdot H(\tau_j), \quad H(\tau_j) = \frac{\int_{-\tau_j}^\infty \varepsilon(T)\cdot e^{-\lambda T}dT}{\int_{-\infty}^\infty \varepsilon(T)\cdot dT}$$

As this equation shows, measuring the course of $a_0(\tau_j)$ offers a possibility for determining the decay constant λ. However, for this it is necessary to know the function $H(\tau_j)$. This is represented by a convolution or faltung integral which cannot be given in a closed form.

Nevertheless, the following consideration shows that despite this difficulty it is possible to determine λ: For $\tau_j \leq 0$, only the right-hand side of the function $\varepsilon(T)$ is integrated in $H(\tau_j)$, whereas the left-hand side is included into the integration only at increasing delay. The newly added contributions of

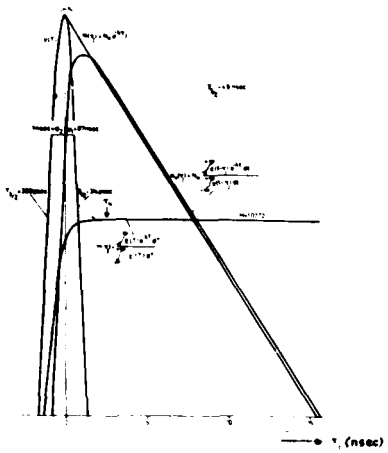

Fig.3 Slope of the Functions $a_0(\tau_j)$ and $H(\tau_j)$.

$\epsilon(T)$ tend to zero for large τ_j, so that $H(\tau_j)$ changes into a constant value H. This means that, for sufficiently large delays τ_j, the coefficients $a_0(\tau_j)$ decrease to a pure e-function whose decay constant is given only by λ. The delay τ_k, from which λ can be determined in this manner, can be defined by an approximate calculation of the function $H(\tau_j)$. Such a calculation was made on an IBM 7090 computer. It was found that, as expected, the magnitude of the delay τ_k depends on the slope of the prompt curve. In addition to the prompt curve, the decay constant λ also enters the value of the constant H, which is plotted in Fig.4. For calculating the function given in this diagram, the prompt curve of Fig.3 was used. Furthermore, Fig.3 shows that the curve $a_0(\tau_j)$ and the simple e-function are displaced parallel to each other. The width of this stagger is determined by the constant H. /14

For a possible fitting of the function $a_0(\tau_j)$ to the test data, this shift is of importance since the compensation must be done in such a manner that the calculated and measured values will coincide for large delays.

If the slope of the prompt curve is known, the function $a_0(\tau_j)$ can be calculated in first approximation; it is then possible to make a fitting for determining λ that considers also the times $\tau_j < \tau_k$. This is of importance because of the fact that these additionally used test points have a smaller statistical error. In such a fitting, the unknown value $\Delta\tau$ of the time zero $\tau_j = 0$ /15

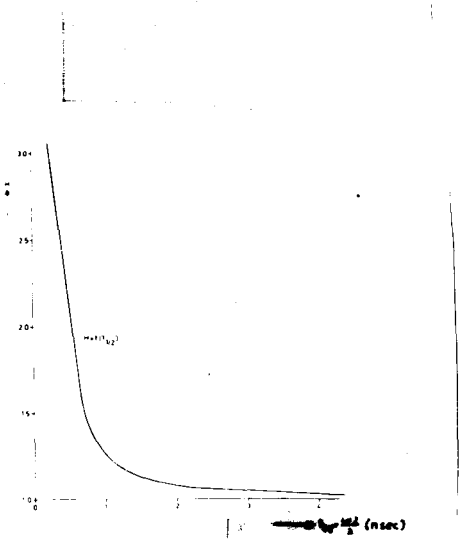

Fig.4 Course of H.

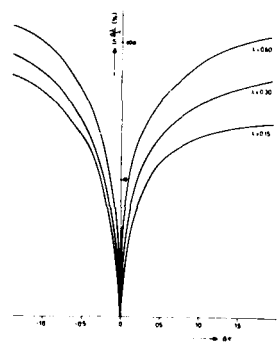

Fig.5 λ as a Function of Δt.

enters the value of λ. In Fig.5, the percentual deviation of the decay constant from its real value is plotted against $\Delta\tau$, in which all test data were fitted.

In addition, the value of λ is further changed if, for calculating $a_0(\tau_j)$, a wrong prompt curve is used. In this case, the influence of the parameters λ_1 and σ_1 is greater than that of λ_2 and σ_2. The reason for this phenomenon is as follows: In the calculation of $a_0(\tau_j)$, the right-hand side of the prompt curve gives the influence of the delays $t < \tau_j$ while the left-hand side allows for the delays $t > \tau_j$. Since the latter occurs less frequently in a nuclear disintegration than the times $t < \tau_j$, the influence of the right-hand side of the prompt curve on the values $a_0(\tau_j)$ and thus also on λ must be greater than that of the left-hand side.

7. Course of the Coefficients $A_k(\tau_j)$

After determining λ, it becomes possible to use the slope of the coefficient $A_k(\tau_j)$ for calculating the magnitude of the attenuation factors λ_k and of the angular correlation coefficients $A_k(0)$. For this, the equation

$$A_k(\tau_j) = A_k(0)\, e^{-\lambda_k \tau_j} \cdot \frac{\int_{-\tau_j}^{\infty} \varepsilon(T)\, e^{-(\lambda+\lambda_k)T}\, dT}{\int_{-\tau_j}^{\infty} \varepsilon(T)\, e^{-\lambda T}\, dT}$$

is used. Here again, the slope of the angular correlation coefficients, for delays $\tau_j > \tau_k$, passes over into a simple e-function. Furthermore, an accurate definition of the prompt curve is not necessary in the case of minor attenuations since, in first approximation, this curve is canceled out from the quotient. Furthermore, in the case of weak attenuations, the e-function can be expanded leading to the following expression: /16

$$A_k(\tau_j) = A_k(0) \cdot e^{-\lambda_k \bar{t}} \quad \text{mit:} \quad \bar{t} = \frac{\int_0^{\infty} \varepsilon(t-\tau_j) \cdot e^{-\lambda t} \cdot t \cdot dt}{\int_0^{\infty} \varepsilon(t-\tau_j) \cdot e^{-\lambda t} \cdot dt}$$

These equations indicate that, after introduction of a $\bar{t}$ axis, the parameters $A_k(0)$ and λ_k are easy to determine graphically. Since the $\bar{t}$ axis differs from the τ axis, the value $A_k(0)$ is located at $\bar{t} = 0$ rather than at $\tau_j = 0$. As will be described in more detail, determination of the time zero point $\tau_j = 0$ encounters difficulties in the measured curves. For the curve fitting, an accurate knowledge of this point is of importance; it was found that this point was

correctly selected only if the fitting furnishes a value $A_k(0)$ for the instant $\bar{t} = 0$.

The physical meaning of the times $\bar{t}$ will be explained below.

8. Mean Delay Time

The existence of a prompt curve has the consequence that gamma quanta whose delay t differs from τ_j may contribute to the number of coincidences $N(\vartheta, \tau_j)$. The contribution probability for each t was given by $\lambda \cdot V(\tau_j - t) \exp(-\lambda t) \cdot W(\vartheta, t, s)$. Thus, the delay which, in measuring $N(\vartheta, \tau_j)$, had existed on the average between the quanta, is defined by the following expression:

$$\bar{t}(\vartheta) = \frac{\int_0^\infty t \cdot \varepsilon(t-\tau_j) e^{-\lambda t} \left(1 + \sum_k A_k(0) e^{-\lambda_k t} P_k(\cos\vartheta)\right) dt}{\int_0^\infty \varepsilon(t-\tau_j) e^{-\lambda t} \left(1 + \sum_k A_k(0) e^{-\lambda_k t} P_k(\cos\vartheta)\right) dt}$$

where $\bar{t}(\vartheta)$ denotes the mean delay time. Since the product $A_k(0) \cdot \exp(-\lambda_k t) \cdot P_k(\cos\vartheta)$ is small with respect to 1, this delay time can be represented also by the simplified expression /17

$$\bar{t}(\vartheta) = \frac{\int_0^\infty t\, \varepsilon(t-\tau_j) e^{-\lambda t}\, dt}{\int_0^\infty \varepsilon(t-\tau_j) e^{-\lambda t}\, dt}$$

If this simplification were not possible, then a calculation of the coefficients $A_k(\tau_j)$ from the three counting rates $N(\vartheta_i, \tau_j)$, $(i = 1, 2, 3)$ would be erroneous since, at each counting rate, a different delay had existed on the average between the gamma quanta. Thus, events would be combined that timewise do not belong together. Therefore, to define accurately in how far the approximation $\bar{t}$ for $\bar{t}(\vartheta)$ is permissible, the function $\bar{t}(\vartheta)$ was calculated in first approximation. For the coefficients $A_k(0)$, a value of 1 was assumed and, for λ_k/λ, a value of 0.4. As shown by a calculation at the angles 90°, 135°, and 180°, the maximum deviation of the function $\bar{t}$ from $\bar{t}(\vartheta)$ is 0.12%. Thus, the approximation is entirely permissible.

9. Integral Attenuation Factor

By means of the differential attenuation factors λ_k, integrally measured angular correlation coefficients can be corrected for attenuation. This is done by the integral attenuation factors G_k whose correlation with the λ_k can be de-

fined by the following considerations: In integral measurements, the time resolution T_R is large in comparison with the lifetime of the intermediate level, so that all delays $t < T_R$ furnish a coincidence signal with equal probability. The prompt curve then changes into a rectangular distribution of constant height A and of length T_R. In this case, the following expression is obtained for the coincidence counting rate:

$$N(\vartheta, \tau_j) = \frac{N_0}{I} \int_0^\infty A e^{-\lambda t} \left(1 + \sum_k A_k(0) e^{-\lambda_k t} P_k(\cos\vartheta)\right) dt$$

$$= 1 + \sum_k A_k(0)\, G_k \cdot P_k(\cos\vartheta)$$

with the integral attenuation factors $G_k = \lambda/(\lambda + \lambda_k)$.

III. DESCRIPTION OF AN INSTRUMENT FOR DIFFERENTIAL MEASUREMENTS OF ANGULAR CORRELATIONS

/18

1. Purpose and Applicability of the Instrument

In this Chapter, an instrument constructed for differential measurement of angular correlations will be described. The conventional arrangement (Ref.2, 14) of two detectors was modified to one with four detectors, which permits a more accurate measurement of the parameters λ, λ_k, and $A_k(0)$.

This equipment, because of the above modification, permits a quadruple simultaneous measurement of one and the same angular correlation, thus furnishing four values for each parameter with which a weighted mean value can be determined. This reduces the statistical error of the results by a factor of 2 in comparison with the conventional arrangement.

These more accurate results are of special interest for the attenuation factors, since the theory by Abragam and Pound permits statements - from the ratio λ_1/λ_2 - as to the type of the perturbing interaction and, in favorable cases, even permits calculation of the moments of excited nuclear levels.

We had originally intended to use the instrument for measuring the attenuation parameters λ_k at nuclear levels whose lifetimes are within the domain of a few nanoseconds. This places strict requirements on the time-resolution properties. First, the half-width of the prompt curve must not be more than a few nanoseconds and, secondly, the flanks must be as steep as possible meaning that the half-value width of their descents must be close to 1 nsec.

2. Detectors

As mentioned before, the slope of the prompt curve is determined almost ex-

clusively by the detectors which, in our case, consisted of NaI(Tl) crystals with attached multipliers. In these detectors, the following factors are of importance for the time resolution: response probability for the incident gamma energy, decay time of the excitation centers, amplification factor, and transit-time fluctuations of the multipliers. The influence of these quantities and /19 of the activity on the slope of the prompt curve had been investigated in detail and discussed by M.Forker (Ref.2).

To reach as great as possible a response probability for high-energy quanta, 3" × 3" NaI(Tl) crystals were used in two of the four detectors. The 14-stage multipliers were of the XP 1040 type manufactured by the Valvo Co., having an amplification factor of 10^8 at 3 kv high voltage applied, and a transit time fluctuation of 1 nsec (Ref.3). For recording low-energy quanta, 1.5" × 2" NaI(Tl) crystals were used in the other two detectors, to which the 14-stage multiplier 56 AVP was connected. These multipliers had a current amplification of 10^8 at a high voltage of 2 kv and a transit time fluctuation of 0.5 nsec (Ref.3).

The decay time of NaI(Tl) scintillators is close to 250 nsec. To obtain detectors with shorter decay times, plastic scintillators can be used whose excitation centers decay with about 10 nsec. The drawback of these types is that they have almost no energy resolution, since their photoelectric response probability is very low. The reason for this lies in the low ordinal number of the plastic material, which permits a detection of gamma quanta only over the Compton effect.

Another possibility for obtaining detectors with rapid decay times is to use NaI crystals without addition of thallium. In these, however, crystal cooling is necessary for obtaining a satisfactory light yield since the optimum light yield is close to 80°K (Ref.15). At this temperature, the crystal has a decay time of 45 nsec. This is by a factor of 5 less than in thallium-activated crystals. Its energy resolution is also better, so that the thallium-free crystals have better properties than the thallium-activated types. Their disadvantage lies in the necessary cooling which necessitates an extensive cooling arrangement (Ref.16) while still requiring light conductors, a fact that might cancel some of the good properties of Tl-free crystals. In the instrument described here, we scheduled the use of Tl-free crystals instead of the 1.5" × × 2" NaI(Tl) scintillators, for which reason a cooling device was additionally /20 installed.

For testing the time resolution of the apparatus, coincidence measurements were made with 511-Kev positron annihilation radiation. We used either a 1.5" × × 2" or a 3" × 8" crystal. These furnished prompt curves whose slopes were close to 350 μμsec and whose half-widths were 1.8 nsec. Other time resolution measurements were reported by K.Krien (Ref.13). In the following Sections, the mechanical and the electronic arrangements of the instrumentation will be described.

3. Mechanical Arrangement

To calculate the ratio λ_4/λ_2, it is sufficient to determine the slope of the coefficients $A_2(\tau_j)$ and $A_4(\tau_j)$. For this, measuring the coincidence count-

ing rate $N(\vartheta, \tau_j)$ at the three angles of 90°, 135°, and 180° is adequate. For producing these three angles, the following arrangement was made: The detectors with the small crystals 1 and 2 make an angle of 90° and are rigidly mounted to a rotary table having a diameter of 1010 mm. The two detectors with the large crystals 3 and 4 are mounted to a sector W which is rotated about the source Q in the table plane by means of a Dunker motor. This motor will be designated as "traction motor" in what follows.

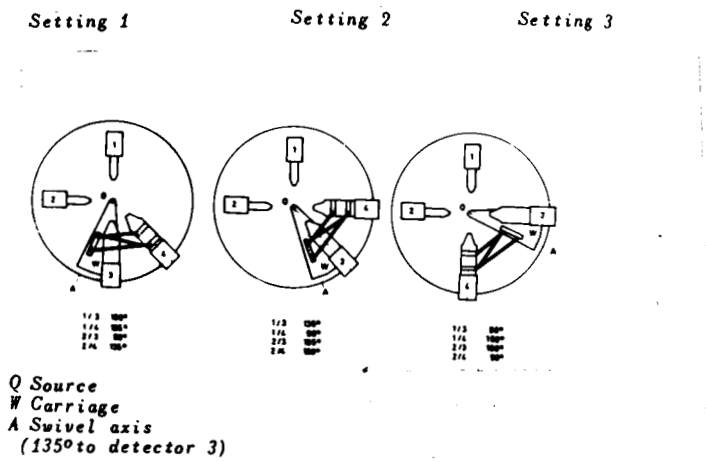

Fig.6 Detector Arrangement.

The reason for the rigid mounting of the two detectors 1 and 2 is the desire, when necessary, to make the small crystals exchangeable for Tl-free NaI scintillators. The cooling device, required in that case, would prevent any shift of the detectors. /21

When the sector W goes through the three positions shown in Fig.6, the three required angles 90°, 135°, and 180° can be established between the detector 3 rigidly connected to the sector and the detectors 1 resp. 2. If the detector 4 were rigidly mounted to W, it would become impossible to form an angle of 180° between this sector and the detector 1 or an angle of 90° with the detector 2. This difficulty can be overcome by swinging the detector 4 over the detector 3 when moving the sector from the setting 2 to 3. This swivel motion is executed about the axis A, which together with the detector 3 includes an angle of 22.5°.

For balancing the weight of the detector 4, a counterpoise displaceable by means of a lever arm (not shown in Fig.6) is attached to the axis. Rotation of this axis, which then is easy to do, takes place over a V-belt by means of a second Dunker motor which will be designated below as "swivel motor". The axis itself can be shifted in the plane of the table, to permit a collimation.

Mounting of the detectors 1 and 2 and of the source is done exactly as described in earlier papers of our research group (Ref.12, 17).

4. Electronics

The electronics of the instrument can be subdivided into five parts: eight coincidence circuits, four peak stabilization circuits, fourteen counters, one multichannel analyzer, and one automatic device for controlling the movements and measuring course.

a) Coincidence Circuits

The instrument requires eight coincidence circuits since, behind the detectors 3 and 4, two single-channel discriminators are mounted which makes it possible to select two powers. This permits simultaneous measurement of two /22
different angular correlations between the detectors 1 and 3 resp. 1 and 4. For this, four coincidence circuits are required. Since, in addition, these two angular correlations are measured also between the detectors 2 and 3 resp. 2 and 4, four additional coincidence circuits are again required. All eight coincidence circuits operate on the fast-slow principle and have exactly the same arrangement. This coincidence principle has been discussed at various occasions (Ref.2, 4, 5).

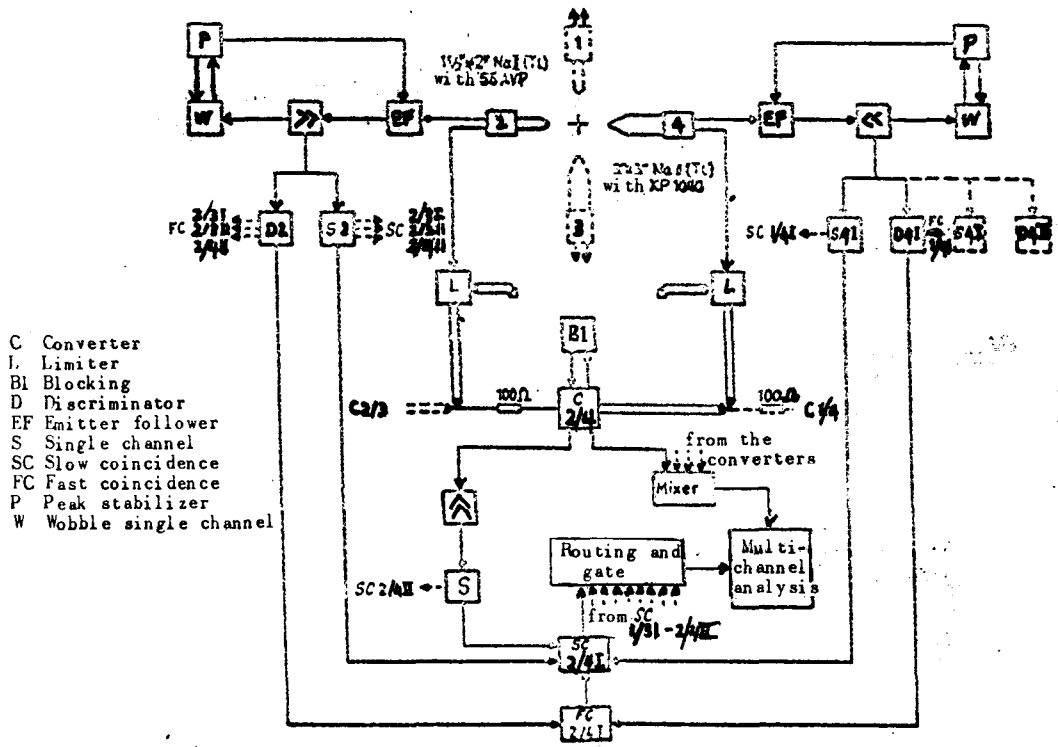

Fig.7 Block Diagram of a Coincidence Circuit.

Figure 7 gives the block diagram of one of the circuits. The electronics used in the slow portion and consisting of amplifiers, single-channel discriminators, and coincidence stages, was purchased from the Cosmic Radiation Laboratories and has been described in detail in an earlier paper by our research group (Ref.12).

As shown in Fig.7, the output signals of the slow coincidence circuits /23
are fed to a routing unit. This triggers the gate of the multichannel analyzer for passing the converter pulse and, simultaneously, ensures that each pulse is

stored in the correct subgroup or register. A paper on the accurate operating mode and the design of this building block as well as on the necessary mixer was published by K.Krien (Ref.13).

To make the eight slow coincidence circuits mutually completely independent, an additional coincidence output was built into the single-channel discriminators of the detectors 3 and 4 (F.C. 1/4I for the detector 4 in Fig.7) which, just as the already present outputs, has a variable delay time and a variable resolving time. Such decoupling of the coincidence circuits was necessary for rendering adjustment of the instrument simpler and more concise.

b) Multichannel Analyzer

Since eight different coincidence counting rates $N(\vartheta, \tau_j)$ are to be measured and since this is done successively on three angles, the multichannel analyzer must have 24 subgroups. So as not to impair the resolving power by too low a channel capacity of these subgroups, 128 channels were used for the size of each subgroup. This required a multichannel analyzer of at least 3072 memory locations. Since such an analyzer was not commercially available, we used a multichannel device with 4096 storage locations. We have scheduled to measure coincidence spectra in the remaining 1028 channels. This would be of great advantage in correcting for admixtures by other energies.

c) Counters

The output pulses of the eight slow coincidence circuits as well as the individual counting rates of the six single-channel discriminators are registered in a counting unit. This is done to correct for accidental coincidences, activity drop, and misalignment of the source. In addition, these counting rates permit calculation of the integral angular correlation, so that the instrument is capable of making differential as well as integral measurements. /24

For recording the individual counting rates, one-megacycle counters are used having a capacity of 10^8 pulses, while the eight counters for the coincidence counting rates operate at 200 kc and have a capacity of 10^5 pulses. These fourteen counters were purchased in one large unit from the Ransom Research Co. This unit permits read-out of the counter contents into a typewriter and, if desired, into a tally tape punch in the IBM code.

d) Peak Stabilization

The conventional method for peak stabilization (Ref.17), consisting in a re-adjustment of the high voltage at the multiplier, could not be used here. Fluctuations in the high voltage produce variations in the transit time of the electrons which may be undesirable when measuring time relations. For this reason, a peak stabilizer was installed which controls the height of the energy pulses without changing the high voltage. Essentially, this is obtained by making one resistance variable at a voltage divider circuit in the emitter follower EF (Fig.7). This resistance is formed by the internal impedance of an in-

candescent lamp, which is dependent on the current. A more accurate description of the peak stabilization has been given by E.Gerdau (Ref.18).

e) Automatic Control

The fully transistorized automatic control unit has two functions; one is to control the machine cycle and the other is to regulate the kinetics of the detectors, which is complicated by the necessary swivel of the detector 4. Both parts of the automatic unit will be described in more detail below.

α) Machine Cycle

The concept of "machine cycle" comprises the following processes: connecting and disconnecting the counters and the multichannel analyzer at the beginning and end of the measuring period; printing of the sector position and the /25 counter contents on typewriters and, if desired, on tape punches.

Timing device. The duration of the measuring time in one sector position can be prescribed by means of a clock or timer. This timing device was purchased from the Phillips Co. and permits setting of 15 time intervals between 1 sec and 4×10^4 sec or between 0.01 min and 4×10^2 min. The accuracy of these intervals is 0.01% and is determined by the tolerance of the 10-kc quartz crystal oscillator which controls the clock.

After the set time has elapsed, the timer produces a pulse which is fed to the connected automatic control unit and resets the clock to zero.

Disconnection of multichannel analyzer and Ransom counters. The signal supplied to the automatic control is branched there and is fed to a trigger or toggle (A61 in Fig.8) and to two flip-flops, designated in Fig.8 by tally-FF resp. by MC-FF. These flip-flops, after being triggered by the clock signal, change their output voltage. This causes interruption of the analyzing process in the multichannel analyzer and closes a gate in the Ransom unit. This gate simultaneously disconnects all fourteen counters. The alternating output voltage of the tally flip-flop trips a mercury relay which connects the motor of the tally tape punch.

Printing of the sector position. The setting at which the respective measurement is taking place is printed on punch tape and typewriter before the fourteen counting rates, in order to check whether - during a given measurement - the sector settings were changed in the correct sequence. This printing is triggered by the clock signal and is done across the toggle A61 - A73. In this case, the toggle A61 is used for delaying the clock signal by 1 sec, for two /26 different reasons: On the one hand, the printing of the sector position is not to be falsified by stray pulses of the cut-in tally motor and, on the other hand, the punch-tape printer will operate correctly only when its motor has reached full rpm. For this, approximately 1 sec is needed.

The signal, delayed by the A61, triggers the toggle A71 which gives off two pulses of 0.3 sec length of opposite polarity. The positive pulse $\overline{t-2}$ is fed

to the Ransom unit and there induces printing of the sector position. The negative signal t - 2 is delayed through the toggle A62 by 0.3 sec and then triggers the toggle A72.

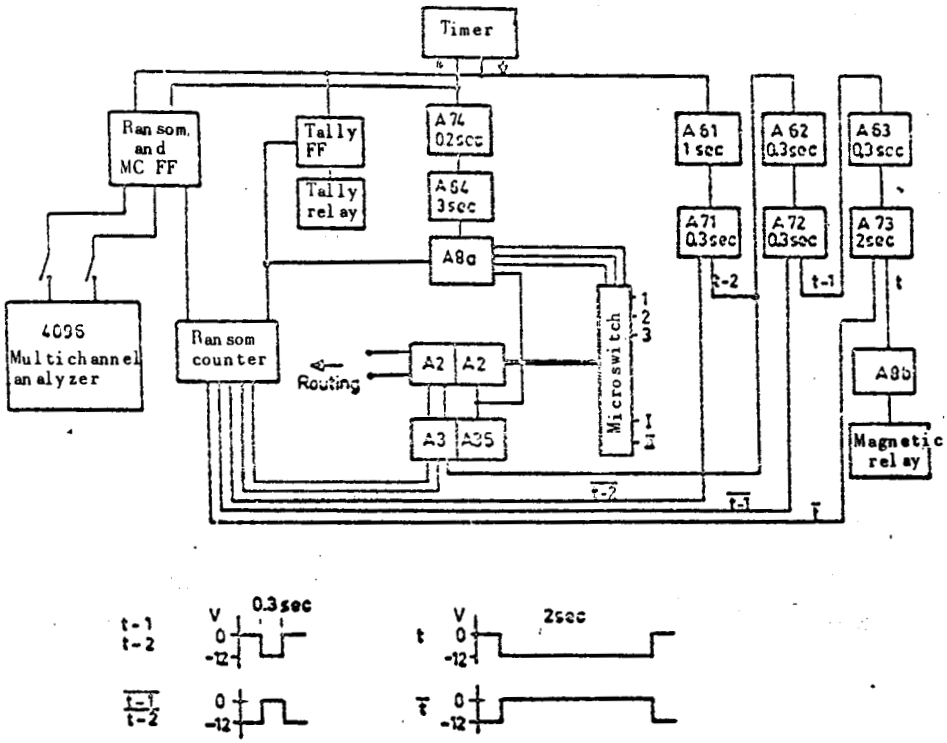

Fig.8 Block Diagram of the Automatic Control Unit.

This toggle or flip-flop furnishes the two output signals $\overline{t-1}$ and t - 1, of which the positive signal in the Ransom unit has two functions: first, that of actuating the tabulator of the typewriter, by which, after printing of the sector position, a spacing to the subsequent counting rates is left. Secondly, a sentinel is punched into the tape, required for later processing of the tape in a computer. The negative signal t - 1 is delayed through the toggle A63 by 0.3 sec and then triggers the toggle A73. /27

The output pulses $\overline{t}$ and t of this flip-flop have a length of 2 sec; of these, $\overline{t}$ instructs the Ransom unit to print all fourteen counter contents, while t causes the sector to change its setting.

Change in sector setting. This change is produced by the traction motor whose circuit is interrupted only when the sector has reached one of its various positions. At this instant, a spring mounted to the sector throws a microswitch mounted to the rotary table. This microswitch - each sector position has one such switch - interrupts the current of the traction motor as long as the switch remains depressed.

The exerted pressure can be canceled by an electromagnet whose circuit is

short-circuited for the length of the pulse t (2 sec). For this, the pulse is passed through the amplifier stage A8b and fed to a mercury relay which closes the circuit of the magnet.

Connecting of the magnet current for 2 sec is sufficient since, during this time, the sector together with the spring has moved so far away from the microswitch that a new throwing of the switch is prevented.

Starting of the timing device. While the sector is moving, both typewriter and tape punch print the contents of all fourteen counters. As soon as, in the obtained setting, the new microswitch is thrown, ground potential is supplied to the stage A8a. This stage is a triple coincidence circuit whose three coincidence conditions are furnished by the following processes: throwing of the new /28 microswitch, termination of printing of the counter contents, and end of swiveling of the detector 4. If these three conditions are met, the output signal of A8a is delayed through the toggle A64 by 3 sec, which triggers the toggle A74.

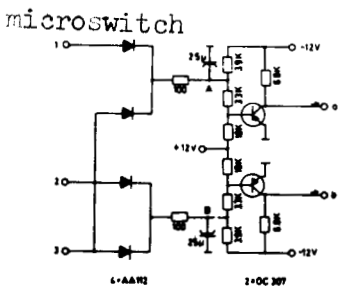

Stage A2

Fig.9 Stage A2.

This output signal has a duration of 0.2 sec and has two functions: It resets the Ransom flip-flop and the MC flip-flop to zero so that a new analysis and counting can be started; in addition, it re-starts the clock.

When moving the sector from position 1 to position 1 resp. from 3 to 3, it may happen that the printing of the counter contents takes longer than this motion. In that case, two coincidence conditions will be present at the stage A8a, if the Ransom unit furnishes the third condition after end of the printing. However, this third condition also triggers the tally flip-flop and thus disconnects the tally motor. Without the 3-sec delay of the output signal through the A8a, the stray pulses of the tally motor would coincide with the opening of the multichannel analyzer and of the counters. This could lead to errors, which are avoided by the delay line A64.

Selection of the Ransom unit; Stage A2. To represent the number of a sector position electronically, the information furnished by throwing of the microswitch is used. This information is converted in the stage A into a binary number, realized at the output by the potential state of the two points a and b (Fig.9).

In this respect, the following data of the microswitch should be given: The switch is a commutator with three external contacts, of which one is connected to ground potential (see Fig.10). This potential is fed to one of the /29 other contacts, depending on whether the microswitch is depressed or not. The contact which, in the depressed state, has ground potential is then connected to the stage A2 which converts the information into the desired binary number. For this purpose, a diode matrix able to convert numbers from 1 to 3 into the binary system is installed at the input. The integrator following the matrix is re-

quired for smoothing since the switch contacts of the microswitch are springy, which superposes parasite oscillations to the output signal of the stage during its rise.

The two transistor loops, following this, are overdriven amplifiers and apply a voltage of 0 v or -12 v to the points a and b. The potential state of these two points then expresses the number of the sector position in binary form, in accordance with the following scheme:

Nr.	a	b
1	-12V	0V
2	0V	-12V
3	-12V	-12V

These output voltages are fed to the stage A3 and to the routing unit.

Stage A3. Printing of the numbers 1 to 3 over the Ransom unit is realized by applying a voltage of -12 v to the corresponding points in the output logic over an OR gate. However, this can be done only at the instant at which the number is to be printed, since otherwise malfunction of the counter contents read-out might occur.

This is the reason for installation of the stage A3. This stage feeds the information from A2 over the number of the sector setting to the OR gate at the instant at which the pulse t - 2 appears, since - simultaneous with this - the pulse t - 2 is generated which triggers the printing. Electronically, A3 consists of a diode coincidence circuit in which the pulse t - 2 furnishes one of the coincidence conditions while -12 v of A2 gives the other condition.

Pulses in the Ransom unit. During the printing on punch tape, an odd /30 number of holes must be produced for each digit in the IBM code. This means that an additional hole must be punched at the number 3. This is known as odd-parity check and, when necessary, must be produced additionally by the signal t - 2. For this reason, the signal is fed not only to the perforator-drive logic and the typewriter logic but also to the odd-parity generator.

The pulse $\overline{t - 1}$ reaches the tabulator logic and carriage-return logic over an OR gate and the typewriter logic over another OR gate.

8) Routing Process

In general, a given measurement starts in the sector position 1. After printing the number of this position on the typewriter and the tape punch, change-over to the position 2 is made. When continuing to position 3, the detector 4 must be swiveled over the detector 3. After this slewing motion is terminated, the swivel motor continues operating for one second to tighten the V-belt. This is to ensure proper position of the detector 4. Its position, whether swiveled or not, is electronically fixed by the two microswitches I and II (see Fig.10). These switches are mounted to the disk which is engaged by the V-belt, and are

thrown by a cam in accordance with the detector position.

In position 3, two measurements are made during which time the polarity of the traction motor and of the swivel motor is reversed between the two measurements. This double return to position 3 is necessary for obtaining an equal number of measurements in all sector positions at the end of a given measurement.

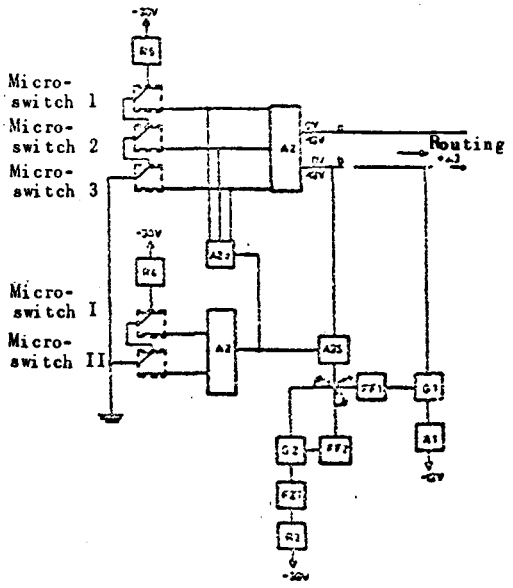

Fig.10 Block Diagram of the Routing Automatic.

On returning to position 2, the swivel motion is reversed in which case the swivel motor again runs for one second longer to tighten the V-belt. Two measurements are again made in position 1, with intermediate pole reversal of the motors.

The portion of the automatic unit, /31 controlling this routing process, operates in accordance with the block diagram shown in Fig.10 and will be described in more detail below.

Position 1 to position 2: So long as none of the microswitches 1 - 3 is thrown, current will flow through the relay R5. This relay is tripped and thus closes the circuit of the traction motor so that the sector will move. The relay is necessary since the traction motor is operated at an alternating voltage of 220 v and the microswitch is unable to switch such voltages.

Position 2: On depressing the switch (2), the current through R5 if interrupted, the relay opens and thus disconnects the traction motor. The ground potential is then fed to the stage A2. The output signal of this stage at the point b is supplied to the double coincidence stage A35 and produces there the first coincidence condition. The second condition is given by the stage A2 of the microswitch I which is depressed at the sector position 2. The throwing of the microswitch 2 thus causes an output signal to appear at the stage A35. The rise edge of the signal triggers the flip-flop 1 (FF1) which causes the gate G1 to open. A green light indicates this opening.

The relay R1, short-circuiting the swivel motor, is so arranged that it will trip only when the point b is at ground potential. This is the case whenever one of the two microswitches 2 or 3 is not depressed.

The output signal of A35 is also fed to the gate G2 and the flip-flop 2 /32 (FF2). In contrast to the FF1, the FF2 does not respond to this rise edge so that the gate G2 remains closed by FF2. For this reason, the flip-flop FZT, which responds to the rise edge, cannot be triggered now. This flip-flop is used for letting the swivel motor, across the relay R2, continue running for one more second.

Position 2 to position 3: Because of the pulse t, the pressure exerted on the microswitch 2 is relieved by means of the electromagnet. This closes the circuit across the relay R5, and the sector begins to move. At the output b of A2, ground potential will now be present; since the gate G1 is now open, the relay R1 can be tripped. This closes the circuit of the swivel motor and swivels the detector 4.

Since the coincidence condition is no longer satisfied for the stage A35, a pulse appears at the output to which the FF2 will respond. This flip-flop is triggered and thus opens the gate G2. As with the other gate, opening of this gate is indicated by a green light. These lights make it possible to decide at the beginning of a given measurement whether the flip-flops FF1 and FF2 had been flipped in the right position. If this is not the case, proper adjustment can be made from the outside.

Position 3: Throwing the switch 3 disconnects the traction motor. The output potential of -12 v at the point b disconnects the current across the relay R1. The circuit of the swivel motor remains closed across the relay R4, since the swiveling takes longer than the travel and since none of the two switches I and II had been depressed during the swiveling. An interruption of the current by the relay R4 takes place only when the microswitch II is depressed at the end of the swivel process.

This again satisfies the coincidence condition at the A35, so that an output pulse is produced. The rise edge of this pulse is now able to trigger the /33 flip-flop FZT, so that the circuit of the swivel motor, across the relay R2, is kept open for the duration of the trigger pulse (1 sec).

In addition, the rise edge also triggers the flip-flop 1, which again closes the gate G1.

Position 3 to position 3: If the microswitch 3 is no longer depressed, the ground potential appearing at the point b can no longer trip the relay R1 since the gate G1 is closed. In addition, the output signal of A35 - with the coincidence condition no longer being satisfied - triggers also the flip-flop FF2 and thus closes the gate G2.

The traveling sector contacts a pole-reversing switch mounted to the rotary table, which changes the direction of the current flowing through both swivel and traction motor by means of a miniature polar relay.

During the return motion, the sector again occupies position 3 and the corresponding microswitch is depressed. This causes A35 to produce a signal which triggers the flip-flop FF1 and thus opens the gate G1. The flip-flop FZT cannot be triggered since G2 is closed.

Position 3 to position 2: Since the gate G1 is open, the swivel motion takes place as soon as the microswitch 3 is no longer depressed. Simultaneously, the FF2 flops back, opening the gate G2. After the swiveling process is terminated, the output signal of A35, across the flip-flop FF1, closes the gate G2 and triggers the flip-flop FZT.

Position 2 to position 1: No swiveling takes place when the switch 2 is no longer depressed, since the flip-flop FF1 keeps the gate G1 closed. The gate G2 is also closed by the output pulse of A35. Throwing of the microswitch 1 has no influence on this part of the automatic unit.

Position 1 to position 1: When the sector moves on from position 1, it again encounters a pole-changing switch which changes the current direction through both motors. The returning sector then resumes position 1. On moving from this position, the entire above-described process begins anew. /34

IV. INTERPRETATION OF A DIFFERENTIAL MEASUREMENT /35

1. Description of the Computer Programing

Processing of a given measurement, for the apparatus described here, can be done only on an electronic computer because of the large volume of data. We used the IBM 7090 computer of the Institute for Instrumental Mathematics of the University Bonn. For this computer, we developed programs for processing the data in three steps.

In the first step, the data of the fourteen counters and the content of the multichannel memory are translated from punch tape to punch cards. For this, we prepared a program which permits a correct translation of the data even if punch-tape errors are present.

In a second step, a second program is used for calculating, from the punch-card data, the course of the coefficients $a_0(\tau_j)$ and $A_k(\tau_j)$ as well as their errors for all eight angular correlations. Corrections are made for drop in counting rate, misalignment, backscattering effects, and accidental coincidences. The mathematical apparatus, forming the basis for these calculations, had been described in an earlier paper of our research group (Ref.12). The calculated coefficients and their errors are printed in tabulated form as well as punched on punch cards. In addition, the coefficients of the integral coincidences (see p.17) are calculated and written out.

In a third step, theoretical curves are fitted to the experimentally determined coefficients, whose slope can be calculated by means of the formulas given in Chapter II. For this, a third program was prepared which will be described in more detail below.

2. Matching Method

First, we will describe the matching method used as basis for our program.

Let L_j be the observed data and let the following be valid:

$$F_j(X_i) - L_j = 0 .$$

Here, the first term represents the functional value of the function $F(X_i)$ /36

at the point j, while X_i are parameters on which this function depends. These parameters are the items to be matched. Since the values L_j as found by observation generally are not free of errors, the following more accurate expression is needed:

$$F_j(X_i) - (L_j+v_j) = 0 .$$

This equation is strictly valid only if the parameters X_i are accurately known. However, in most cases only their approximation Y_i is known, so that also the parameters must be given small increments ΔY_i to have the equation remain strictly valid:

$$F_j(Y_i+\Delta Y_i) - (L_j+v_j) = 0.$$

It is now assumed that the improvements of the parameters are so small that their squares can be neglected. A Taylor expansion, which then becomes possible, yields the equation

$$F_j(Y_i) + \sum \frac{\partial F_j}{\partial Y_i} \Delta Y_i - L_j = v_j.$$

Using the abbreviations

$$\frac{\partial F_j}{\partial Y_i} = Z_{ij} \ , \ F_j(Y_i) - L_j = \ell_j$$

we obtain the equation

$$\sum_{j=1}^{W} Z_{ij} \cdot \Delta Y_i + \ell_j = v_j.$$

Here, the subscript j ranges from 1 to a number W that gives the number of observational data. A matching of the parameters is possible only if their number P is smaller than W. In this case, an overdetermined system of equations exists for ΔY_i, which can be uniquely solved by adding a minimum condition. This condition consists in the requirement that the increments v_j are to form a minimum.

Stated more accurately, the least-square deviations $\sum_{j=1}^{W} v_j^2 = [vv]$ must become minimal. This yields the system of so-called normal equations:

$$\frac{\partial [vv]}{\partial \Delta Y_j} = \sum_{K=1}^{W} \left(\sum_{i=1}^{P} Z_{ij} Z_{iK} \right) \cdot \Delta Y_K + \sum_{i=1}^{P} Z_{ij} \ell_i = 0 \quad (j = 1, \cdots, W)$$

$$\text{or:} \quad \sum_{K=1}^{W} r_{jK} \cdot \Delta Y_K + D_j = 0.$$

If the calculated increments ΔY_i are added to the initial values Y_i, new values /37
for the parameters are obtained, with which the calculation can be repeated. This leads to an iteration process which can be terminated as soon as the increments drop below a certain value.

This matching method can be expanded if the errors of the observational data are to be taken into consideration. In that case, a weighted matching is performed, in which the square of the reciprocal error of an observational value is used as its weight P_j. With the aid of these weights, new normal equations are obtained which are derived from the old equations on multiplication by the weights.

The error of the matched parameters is composed of an error determined by the statistical accuracy of the test data and of another error due to the scatter of the test data. The error due to the statistics can be calculated according to the formula $\Delta_i = \sqrt{(r_{ii})^{-1}}$, where $(r_{ii})^{-1}$ represent the elements of the diagonals of the matrix reciprocal to (r_{ik}).

The error due to the scattering reads

$$\sigma_i = \sqrt{\frac{\sum_{j=1}^{N} P_j e_j^2}{-(P-W)}} \cdot \Delta_i .$$

3. Matching of the Coefficients $a_0(\tau_j)$

a) Calculation of the Differential Quotients

The theoretical slope of the coefficients $a_0(\tau_j)$ is given by the formula

$$a_0(\tau_j) = \frac{N_0}{I} e^{-\lambda\tau_j} \int_{-\tau_j}^{\infty} \varepsilon(T) e^{-\lambda T} dT .$$

The parameters to be matched are the decay constant λ and the norming factor N_0 which latter must be so adapted during the calculation that the theoretical curve and the test data coincide for large delays (see p.10).

These delays are realized in our experiment by the channel number of the multichannel analyzer and thus are capable only of discrete values. Therefore, it is entirely possible that the time zero point does not coincide with a channel number. For this reason, the following mathematical argument is derived for the time axis: /38

$$\tau_j = (\beta + j - 1)\cdot\Delta\tau \qquad \tau_j \leq 0$$
$$\tau_j = (\beta - 1)\cdot\Delta\tau \qquad \tau_1 > 0.$$

Here, $\Delta\tau$ is the time interval (for example, in nanoseconds) between two channel numbers, while the parameter β, in units of $\Delta\tau$, indicates the distance of the time zero from the first channel number at which $\tau_j > 0$.

Experimentally, this point can be determined by measuring the prompt curve at the same instrument setting at which the measurement had been made. On the other hand, it might happen that, in measuring on a cascade, prompt coincidences

of other transitions are included so that a prompt curve is established near the time zero, by means of whose maximum the time zero can be determined.

However, the zero point can be determined more accurately by including β as a third parameter into the matching calculation. For this, the three differential quotients Z_{j1} must be calculated, for which the following equations are obtained:

$$\frac{\partial a_0(\tau_j)}{\partial N_0} = Z_{j1} = \frac{1}{I}\int_{-\tau_j}^{\infty} \varepsilon(T) e^{-\lambda(T+\tau_j)} dT, \quad \frac{\partial a_0(\tau_j)}{\partial \lambda} = Z_{j2} = -\frac{N_0}{I}\int_{-\tau_j}^{\infty} (T+\tau_j)\varepsilon(T) e^{-\lambda(T+\tau_j)} dT$$

$$\frac{\partial a_0(\tau_j)}{\partial \beta} = Z_{j3} = \frac{N_0}{I}\left\{\varepsilon(-\tau_j) - \lambda\int_{-\tau_j}^{\infty} \varepsilon(T) e^{-\lambda(T+\tau_j)} dT\right\}.$$

b) Approximate Calculation of the Integrals

It is impossible to represent the faltung integrals, occurring in the calculation of differential quotients, in a closed form; consequently, an approximation method must be used for their determination. This method consists in replacing the reflected prompt curve $\varepsilon(t - \tau_j)$ by a step function, which makes /39 it possible to resolve the faltung integral into a sum of calculable integrals.

For this, the transformation $t - \tau_j = T_I$ is introduced, and the new time axis is subdivided into intervals of a length ΔT. Within these intervals which have the form $\langle T_I - \frac{\Delta T}{2}, T_I + \frac{\Delta T}{2} \rangle$ the reflected prompt curve is considered as constant and the value $\varepsilon_I = \varepsilon(T_I)$ is substituted for the constant. This yields

$$\int_{\tau_j}^{\infty} \varepsilon(T_I) e^{\lambda(T_I+\tau_j)} dT_I = \sum_{I=K}^{N} \int_{T_I-\frac{\Delta T}{2}}^{T_I+\frac{\Delta T}{2}} \varepsilon_I e^{-\lambda(T_I+\tau_j)} dT_I = \frac{e^{\lambda\frac{\Delta T}{2}} - e^{-\lambda\frac{\Delta T}{2}}}{\lambda} \sum_{I=K}^{N} \varepsilon_I e^{-\lambda(T_I+\tau_j)}$$

$$\int_{-\tau_j}^{\infty} (T_I+\tau_j)\varepsilon(T_I) e^{-\lambda(T_I+\tau_j)} dT_I = \frac{e^{\lambda\frac{\Delta T}{2}} - e^{-\lambda\frac{\Delta T}{2}}}{\lambda} \sum_{I=K}^{N} (T_I+\tau_j)\varepsilon_I e^{-\lambda(T_I+\tau_j)}$$

where N is the number of points of the prompt curve of T_1. For determining the values ε_I, the formulas for the prompt curve can be used (p.7), if a time axis, reflected at the neutral point, is used in the calculation. Such an axis is obtained by the argument $T_I = (-\alpha + I - 1) \cdot \Delta T$. In this formula, the quantity α was taken from the prompt curve where this quantity gives the distance between

T = 0 and an instant $T_a > 0$. Here, T_a is determined in such a manner that, at this instant, the prompt curve is already very small relative to its maximum. The minus sign in front of the parameter α furnishes the desired time reflection.

When using the given approximation formula for the faltung integral, caution must be exerted in determining the start of summation K. It might happen that, in the neighborhood of the zero point, the expression $\tau_j + T_i = t$ becomes smaller than zero. This means that the function $\epsilon(T)$ at the point τ_j allows also for contributions due to negative delays between the gamma quanta, which would have no physical meaning. Therefore, K must be so selected that $\tau_j + T_k \geq 0$. For small times τ_j, this means that, in integrating over I, a portion of the function $\epsilon(T_I)$ is omitted. This portion is shown hatched in Fig.11. For K, this /40 yields

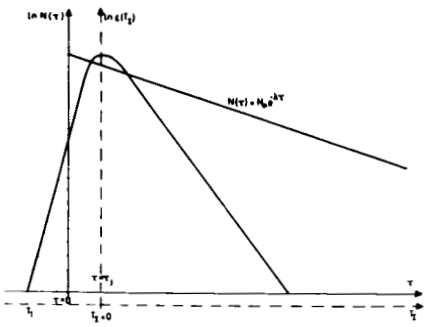

Fig.11 For Selecting K.

$$\tau_j + T_K \geq 0, \quad T_K = T_1 + (K-1)\cdot\Delta T$$

$$\Rightarrow K \geq 1 - \frac{T_1 + \tau_j}{\Delta T} = S$$

$$K = [S].$$

The bracket around S means that, for K, the smallest integer which is larger or equal to S must be taken. This furnishes the following final expressions for the differential quotients:

$$Z_{j1} = a_j = L \sum_{I=[S]}^{N} \epsilon_I e^{-\lambda (I-S)\cdot\Delta T}, \quad Z_{j2} = b_j = -N_0 L \sum_{I=[S]}^{N} (I-S)\cdot\Delta T \cdot \epsilon_I e^{-\lambda (I-S)\Delta T}$$

$$Z_{j3} = g_j = N_0 \left\{ \frac{1}{I} \epsilon(-\tau_j) - \lambda Z_{j1} \right\}$$

with: $$L = \frac{e^{\lambda \frac{\Delta T}{2}} - e^{-\lambda \frac{\Delta T}{2}}}{I \cdot \lambda}.$$

4. Matching of the Coefficients $A_k(\tau_j)$

The theoretical slope of these coefficients is given by the equation

$$A_K(\tau_j) = \frac{A_K(0)\cdot\int_{-\tau_j}^{\infty}\varepsilon(T_I)\cdot e^{-(\lambda+\lambda_K)\cdot(T_I+\tau_j)}\,dT_I}{\int_{-\tau_j}^{\infty}\varepsilon(T_I)\cdot e^{-\lambda\cdot(T_I+\tau_j)}\,dT_I}.$$

The parameters to be matched are $A_k(0)$ and λ_k in this case. The already matched parameters λ and β are used furthermore in the calculation. The required differential quotients can be calculated by means of the following formulas:

/41

$$\frac{\partial A_K(\tau_j)}{\partial A_K(0)} = Z_{j1} = \frac{\int_{-\tau_j}^{\infty}\varepsilon(T_I)e^{-(\lambda+\lambda_K)(T_I+\tau_j)}\,dT_I}{\int_{-\tau_j}^{\infty}\varepsilon(T_I)e^{-\lambda(T_I+\tau_j)}\,dT_I}; \quad \frac{\partial A_K(\tau_j)}{\partial A_K(0)} = Z_{j2} = -\frac{A_K(0)\int_{-\tau_j}^{\infty}(T_I+\tau_j)\varepsilon(T_I)e^{-(\lambda+\lambda_K)(T_I+\tau_j)}\,dT_I}{\int_{-\tau_j}^{\infty}\varepsilon(T_I)e^{-\lambda(T_I+\tau_j)}\,dT_I}.$$

In the interpretive programing, described below, we provided also for the case that the slope of the coefficients $A_k(\tau_j)$ shows a superposition of two e-functions. In this case, the equation for $A_k(\tau_j)$ is expanded in the form

$$A_K(\tau_j) = \sum_{e=1}^{2}\frac{A_{Ke}(0)\cdot\int_{-\tau_j}^{\infty}\varepsilon(T_I)\cdot e^{-(\lambda+\lambda_{Ke})(T_I+\tau_j)}\,dT_I}{\int_{-\tau_j}^{\infty}\varepsilon(T_I)\cdot e^{-\lambda(T_I+\tau_j)}\,dT_I}.$$

In this event, the four parameters $A_{k1}(0)$, $A_{k2}(0)$, λ_{k1}, and λ_{k2} must be matched, for which the following four differential quotients are required:

$$\frac{\partial A_K(\tau_j)}{\partial A_{K1}(0)} = C_j = D_1\sum_{I=[S]}^{N}\varepsilon_I e^{-(\lambda+\lambda_{K1})(I-S)\Delta T}; \quad \frac{\partial A_K(\tau_j)}{\partial \lambda_{K1}} = e_j = -D_1 A_{K1}(0)\sum_{I=[S]}^{N}(I-S)\varepsilon_I e^{-(\lambda+\lambda_{K1})(I-S)\Delta T}$$

$$\frac{\partial A_K(\tau_j)}{\partial A_{K2}(0)} = d_j = D_2\sum_{I=[S]}^{N}\varepsilon_I e^{-(\lambda+\lambda_{K2})(I-S)\Delta T}; \quad \frac{\partial A_K(\tau_j)}{\partial \lambda_{K2}} = f_j = -D_2 A_{K2}(0)\sum_{I=[S]}^{N}(I-S)\varepsilon_I e^{-(\lambda+\lambda_{K2})(I-S)\Delta T}$$

$$D_e = \frac{e^{-(\lambda+\lambda_{Ke})\frac{\Delta T}{2}} - e^{-(\lambda+\lambda_{Ke})\frac{\Delta T}{2}}}{\lambda\cdot I_1\cdot a_j}; \quad I_1 = \int_{-\infty}^{+\infty}\varepsilon(T)\,dT.$$

5. Matching Program

The computer program for performing the mentioned calculations is able to provide for simultaneous matching of eight angular correlations. The program consists of one main program and seven subprograms or subroutines.

The main program is subdivided into five independent sectors; in the first, all necessary data and control signals are written into a part "A". These are /42 read out in the part "B", for control. The second sector, using the subroutine "PROMPT", calculates in the part A the function $\epsilon(T)$ for each angular correlation to be matched. In the part B, the τ_j-axis is calculated for each measurement, for which an estimated approximation value for β had been read in. The differential quotients a_j, b_j, and g_j are calculated in part A of the sector 3, after which the normal equations are derived. For this, the subroutine "INTEGR" is used, which performs the approximate calculation of the integrals by means of the described summation. Matching of the time zero, i.e., calculation of the g_j, can be disconnected as desired, which will be necessary whenever a prompt stray is present. In this case, a zero-point matching is impossible since this would require a matching to points not farther away from the zero point than the maximum width of the prompt curve.

In addition, the mean delay time $\bar{t}$ is calculated; for this, an approximation formula similar to that for the differential quotient can be given.

The sector B calculates the differential quotients c_j and e_j or - if desired - also d_j and f_j, after which the normal equations are derived. In this sector, computation is started only after the matching to $a_0(\tau_j)$ is terminated, i.e., after λ and possibly also β are accurately known.

In the sector 4, part A solves the system of normal equations which is determined by a_j, b_j, g_j. The solution is performed by matrix inversion, making use of the subroutine LEQ. If the zero-point matching has been disconnected, only the system formed by a_j and b_j will be solved. In this same part, after calculating the increments, the relative variations $\frac{\Delta N_0}{N_0}$, $\frac{\Delta\lambda}{\lambda}$, $\frac{\Delta\beta}{\beta}$ are compared with the introduced values, for each angular correlation to be matched. If the relative changes do not drop below these values, the program returns to part 2B where it starts with a new calculation of the τ_j-axes. For all angular correlations whose relative changes have dropped below the accuracy threshold, the iteration is terminated.

At the instant at which the iteration has ended for all angular correla- /44 tions, the computation is continued in part 3B. Here, the differential quotients o_j and e_j as well as, if desired, d_j and f_j are calculated for matching to the coefficients $A_k(\tau_j)$.

These are solved in the sector 4, part B, using the LEQ program. In this portion, interrogation of the relative variations takes place. After terminating the iteration, computation is continued in the sector 5.

In this sector, the errors due to scattering and statistics are first

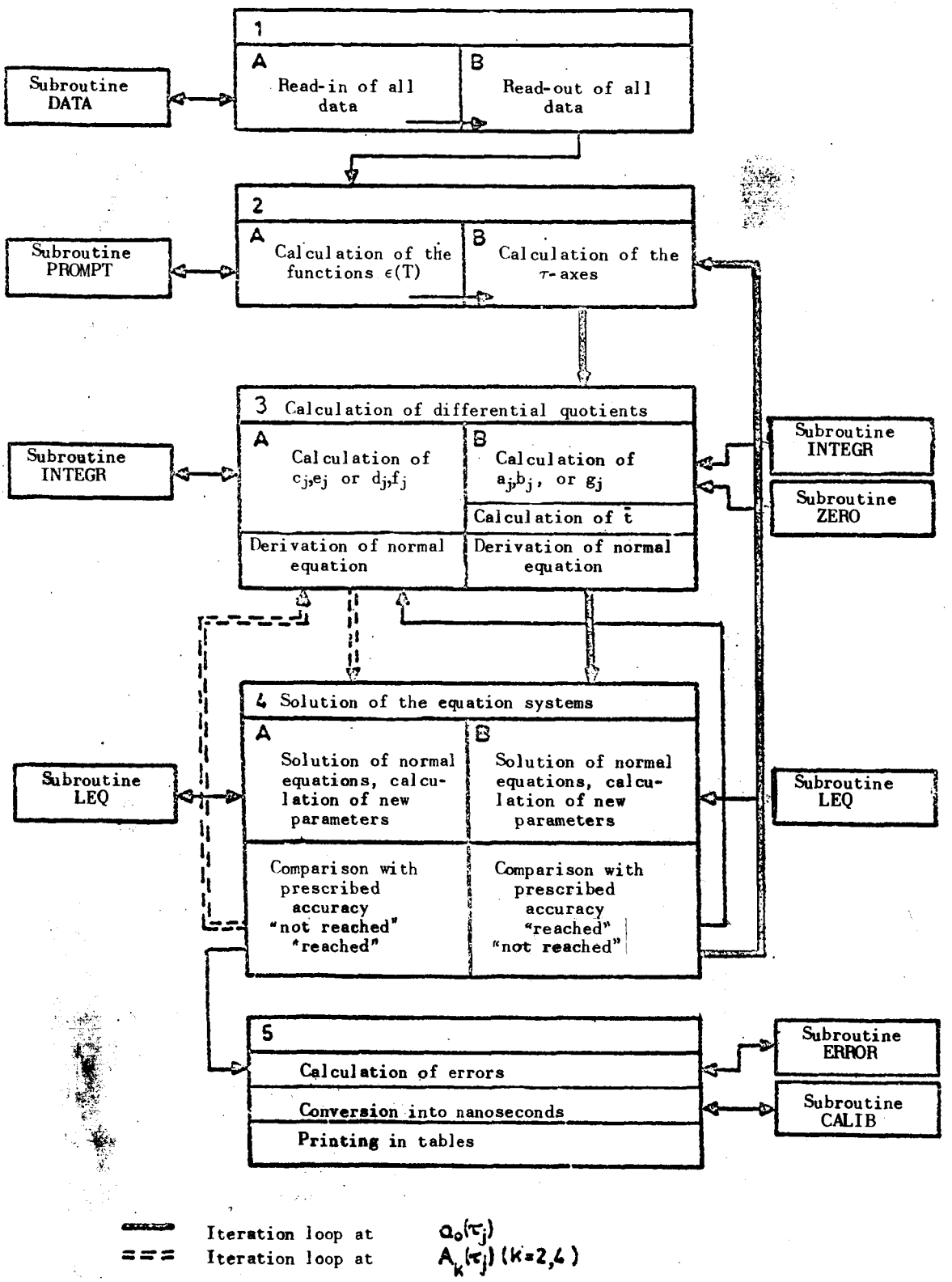
1
A
Read-in of all data
B
Read-out of all data
Subroutine DATA
2
A
Calculation of the functions ϵ(T)
B
Calculation of the τ-axes
Subroutine PROMPT
3 Calculation of differential quotients
A
Calculation of c_j, e_j or d_j, f_j
B
Calculation of a_j, b_j, or g_j
Calculation of t̄
Derivation of normal equation
Derivation of normal equation
Subroutine INTEGR
Subroutine INTEGR
Subroutine ZERO
4 Solution of the equation systems
A
Solution of normal equations, calculation of new parameters
B
Solution of normal equations, calculation of new parameters
Comparison with prescribed accuracy "not reached" "reached"
Comparison with prescribed accuracy "reached" "not reached"
Subroutine LEQ
Subroutine LEQ
5
Calculation of errors
Conversion into nanoseconds
Printing in tables
Subroutine ERROR
Subroutine CALIB
Iteration loop at $a_0(\tau_j)$
Iteration loop at $A_k(\tau_j)$ (k=2,4)

Fig.12

computed, using the subroutine ERROR. By means of the subroutine CALIB, the decay constant and attenuation factors can then be converted into time units (for example, nanoseconds) with the aid of known calibrations of channel units. In the remaining portion of the sector 5, the results are then printed out in the form of tables with headings.

In the entire matching computation, the point from which matching is to start as well as the point at which matching is to stop can be given for each angular correlation.

V. MEASUREMENTS ON YTTERBIUM-172 /45

1. The 1095-Kev Transition in Yb^{172}

In earlier work done by our research group, we used the angular correlation technique for making investigations on Yb^{172} (Ref.17, 19). In this, we made an attempt to determine the mixing ratio of the 1095-Kev transition. Since the spins of the participating level are known, this transition should contain an M1 and an E2 component.

Measurements of the angular correlation on the 1095-79 Kev and the 91-1095 Kev cascades yielded $\delta = 10.3 \pm 2.3$ and $\delta = 0.275 \pm 0.025$ as solutions for the sought mixing parameter.

Since the 203-Kev transition exists as a crossover within a rotation band of pure E2 radiation, the theoretical angular correlation coefficients of the 203-1095 Kev cascade can be calculated by means of the indicated mixing parameters. These are as follows:

$A_2 = -0.013 \pm 0.009$	$A_2 = -0.148 \pm 0.019$
$A_4 = -0.0135 \pm 0.0000$	$A_4 = -0.0010 \pm 0.0004$
$\delta = +10.3 \pm 2.3$	$\delta = +0.275 \pm 0.025$.

An experimental determination of these coefficients is carried out over an analysis of coincidence spectra, recorded with a two-detector instrument (Ref.17). The result could not be reconciled with any of the theoretical values, since the measured A_2 was located exactly between the above-given values and since an A_4 differing from zero could not be measured outside the error limits.

In measuring the 203-1095 Kev angular correlation, it must always be taken into consideration that a strong Compton component of higher energetic quanta is located below the 203-Kev line, which falsifies the result. In this case, a differential measurement has the advantage over the integral method that, in its interpretation, the perturbing Compton background of the prompt transitions can be eliminated. For this reason, it seemed logical to make a repeat determination of the coefficients of the 203-1095 Kev cascade, by means of the described instrumentation. For this, three measurements were made, which will be described below.

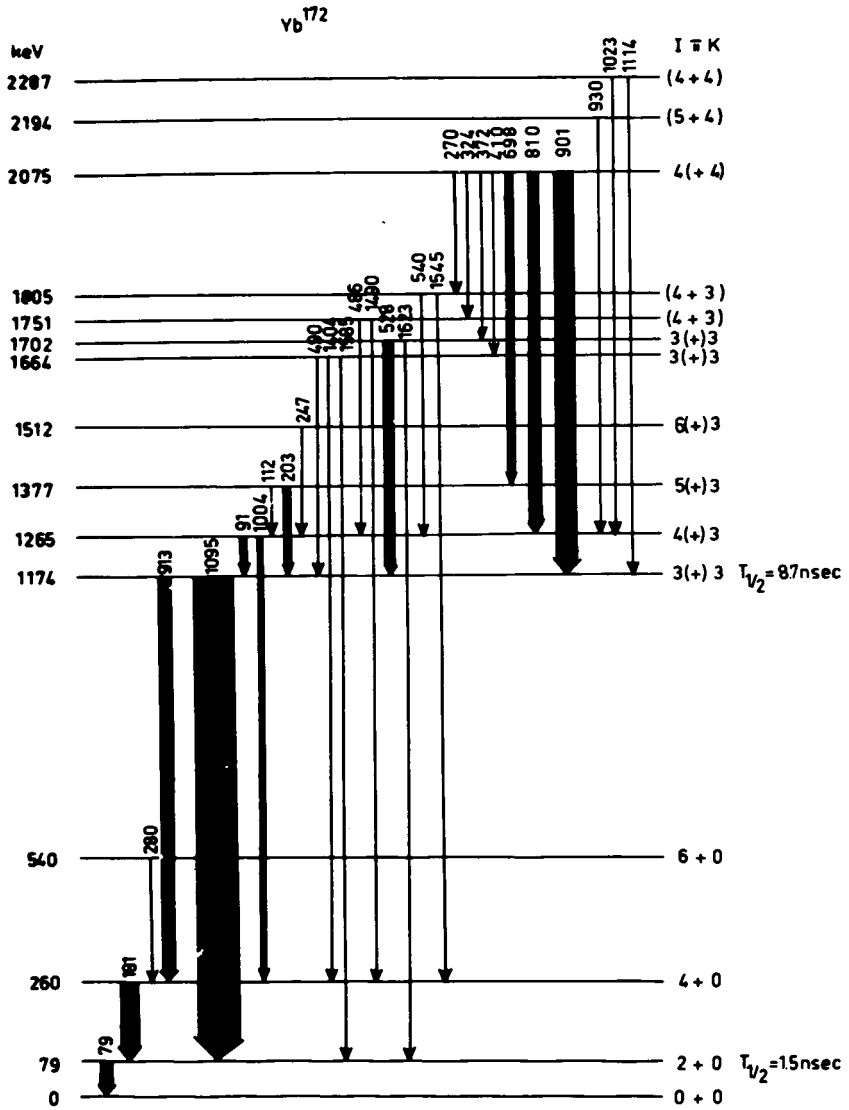

Fig.13 Decay Scheme of Ytterbium-172, according to Harmatz et al. (Ref.23).

2. Differential Measurement of the 203-1095 Kev Cascade /47

The specimen required for this measurement was prepared in the cyclotron of our Institute, by a (d, 2n) reaction:

$$Yb^{172}\ (d,2n)\ Lu^{172}\ .$$

The source used consisted of $LuCl_3$, dissolved in 0.1N HCl. Figure 14 gives the energy spectrum, recorded with a 1.5″ × 2″ NaI(Tl) crystal. For detecting the 203-Kev quanta, the detectors 1 and 2 with the small crystals were used, whose single-channel window was adjusted to the right-hand edge of the 181, 203 Kev double peak. Since the intensity ratio of the two lines was not accurately known, a more accurate adjustment to the 203-Kev line was impossible.

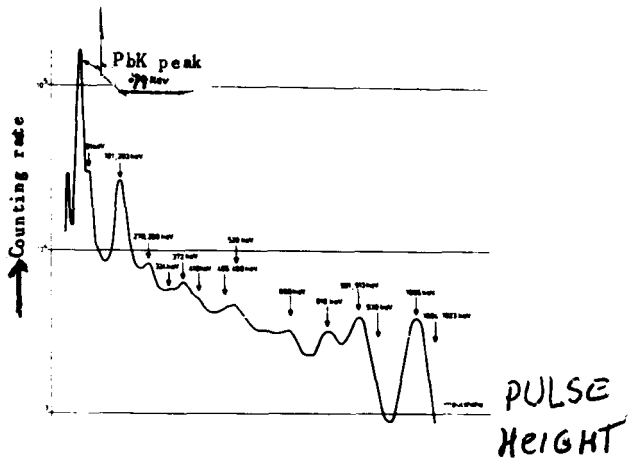

Fig.14 Energy Spectrum of Ytterbium-172.

The recording of the high-energy quanta was done by means of the detectors 3 and 4 which were especially suitable for this because of their large 3″ × 3″ NaI(Tl) crystals. Since only one angular correlation was to be measured, the use of a single-channel discriminator was sufficient for these detectors, so that only four coincidence circuits were needed. Therefore, 12 subgroups are sufficient for this measurement even in the multichannel analyzer, for which reason these subgroups could be increased from 128 to 256 channels.

The total measuring period was 15 days within which the angles were changed every 1000 sec by varying the sector position. In addition, the single-channel settings were checked every 3 days, making an intermediate evaluation by /48 means of the described programs. In matching, all points for which the delay was less than 4 nsec were disregarded, so that the interfering prompt coincidences had no influence on the value of $A_2(0)$ and $A_4(0)$.

Prompt coincidences are produced by the fact that, at the indicated energy setting, other cascades are also covered. These comprise the 1404, 1410, and 1545-Kev transition to the 260-Kev level, which all are in prompt coincidence with the sharp 181-Kev line and can be detected, over the Compton effect, in the 1095-Kev window of the detectors 3 and 4, whereas the 181-Kev line shows strong components in the 203-Kev window of the detectors 1 and 2. In addition, the 1023-1004 Kev cascade furnishes prompt coincidences since the 1023-Kev line is also located in the 1095-Kev window and the 1004-Kev transition can be detected over the Compton effect in the detectors 1 and 2. This detection is made easier

because of the fact that the backscatter peak of this line is located near 200-Kev. Other prompt components are furnished by the following cascades:

270 - 1545 Kev, 324 - 1490 Kev, 372 - 1404 Kev, 410 - 1404 Kev.

In all, the component of prompt coincidences is 35% ± 5%. A determination of the anisotropy of this component, with respect to the prior integral measurement, was unnecessary since correction had been made for all perturbing strays either of the retarded or prompt type.

The result of the measurement comprises the following four values $A_2(0)$ which have not yet been corrected for the finite aperture angles of the detectors:

-0.063 ± 0.012 -0.050 ± 0.012 -0.058 ± 0.009 -0.050 ± 0.011.

Figure 15 gives these values and their errors; they coincide within the error limits. For a later interpretation, the two $A_2(0)$ values, measured by the detector 1 respectively the detector 2, were weighted and averaged. These mean values are as follows:

Detector 1: $\overline{A_2(0)} = -0.056\pm0.008$
Detector 2: $\overline{A_2(0)} = -0.055\pm0.007$.

For $A_4(0)$, the values were /49

Detector 1: $\overline{A_4(0)} = -0.007\pm0.008$
Detector 2: $\overline{A_4(0)} = +0.003\pm0.008$.

3. Differential Measurement of the Compton Background with the 1095-Kev Transition

The values for the sought coefficients, measured in this manner, must be corrected for the Compton strays of all transitions that end on the 1174-Kev level and thus are in delayed coincidence with the 1095-Kev line. This necessitated a differential measurement of the angular correlation of the Compton background, located below the 203-Kev peak.

For this, the single-channel windows of the detectors 1 and 2 were adjusted to the Compton background at 300 Kev. This point was selected because of the fact that the broadest single-channel setting is possible there, which is of importance because of the low counting rate of the background. The error produced by the fact that the contribution of the 270-Kev transition was not measured, can be neglected since the Compton trough of this line is located exactly below the 203-Kev peak.

The background measurement took 14 days, in which the sector position was changed every 1000 sec. The four individual values for $A_2(0)$ and the weighted mean value are shown in Fig.15. The values for the background coefficients, not corrected for the aperture angle, read as follows:

$$\overline{A_2(\delta)} = -0.054 \pm 0.007 \quad ; \quad \overline{A_4(\delta)} = -0.000 \pm 0.010.$$

The magnitude of the error is due mainly to the statistics which, because of the reduced activity of the sample, was not very high. However, it can be estimated that a reduction of the error by half will lead to an improvement of not more than 1% in the inaccuracy for the sought A_2. This is due to the fact that, in the error calculation to be made, the main factor entering as denominator is the difference between the Compton component and the component of the 203-Kev line. The magnitude of these components will have to be determined in a third measurement. /50

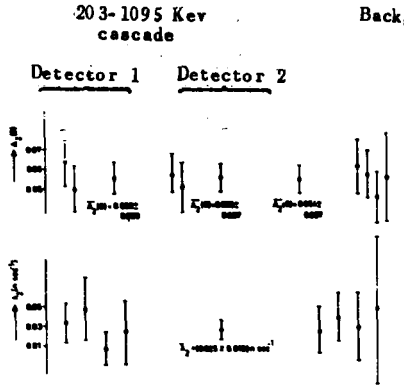

Fig.15 Result of First and Second Measurement.

4. Recording a Delayed Coincidence Spectrum

This third measurement consisted in recording, by means of the 1095-Kev line, a coincidence spectrum delayed by 8 nsec, for the detectors 1 and 2. Such a measurement makes it possible that only those transitions appear in the spectrum that end at the 1174-Kev level and thus interfere with the measurement on the 203-Kev line. This line itself occurs without strays from the 181-Kev peak, which facilitates an accurate determination of the various components.

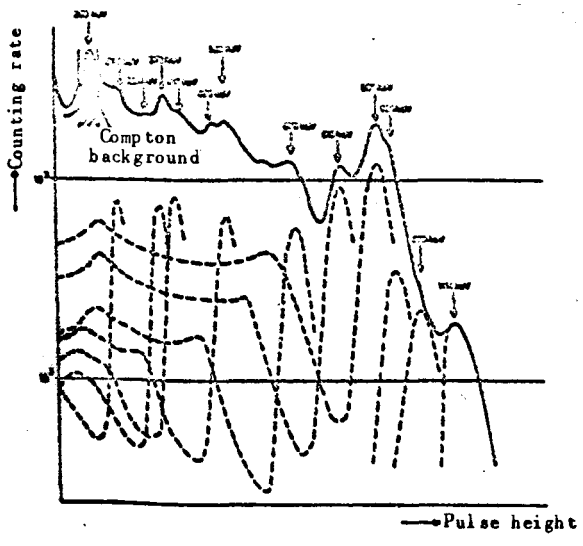

Fig.16 Delayed Coincidence Spectrum of Ytterbium-172, for the Detector 1 with Single-Channel Setting and Individual Spectra.

As a typical example, Fig.16 shows a delayed coincidence spectrum of the detector 1. Here, the single-channel adjustment to the 203-Kev line is shown as a hatched area. To determine the accurate course of the Compton background below the 203-Kev peak in this spectrum, it was neces- /51 to make a spectral analysis. This was done with a computer program developed by W.Rothenburger (Ref.20). The necessary reference spectra were furnished by the nuclei: Co^{60} (1170 Kev), Mn^{54} (840 Kev), Cs^{137} (662 Kev), Na^{22} (511 Kev), and Hg^{203} (279 Kev).

As indicated by the intensity ratio of the 372-Kev and the 410-Kev line, the analysis in the energy region between 200 and 500 Kev is not too good

since, in this region, no suitable reference lines were available.

For the ratio of 203-Kev to Compton component, the interpretation yielded the following values:

Detector 1: 923/2227 = 0,414 ; Detector 2: 1229/2253 = 0,545.

The larger ratio for the detector 2 can be explained by the fact that the setting of the single-channel window to the 203-Kev line was more favorable here, so that a larger segment was covered by the area below the peak.

The accuracy of the two above ratios, because of the low number of reference lines available, is not more than 20%.

The results of the three measurements are compiled in the following calculation:

Let P1 be the component of the 203-Kev line and let P2 be that of the Compton background. Then, the following argument can be established for the sought A_k:

$$A_k(203\text{-}\dots) = \frac{(P1+P2)A_k(\text{meas.}) - P2\cdot A_k(\text{backgr.})}{P1}$$

and for the corresponding error:

$$(\Delta A_k)^2 = \frac{1}{P1^2}\left[(P1+P2)^2\Delta A_k(\text{meas.})^2 + P2^2\Delta A_k(\text{backgr.})^2 + \right.$$
$$\left. + \frac{1}{P1^2}\left[A_k(\text{meas.})^2 - A_k(\text{backgr.})^2\right]\Delta P1^2 + P2^2\Delta P1^2\right].$$

It is obvious that the error is not greatly influenced by the inaccuracy of the analysis, since the measurement showed that A_k (meas.) $\approx A_k$ (backgr.).

Conversely, the influence of the component P1 of the 203-Kev line is very large since it is located in the denominator of the error. Since this component is small because of the high Compton background, a large error must be expected. Computation with the measured values and the indicated formulas yields the following values for the sought coefficients: /52

$$A_2 = -0,065 \pm 0,021 \qquad A_4 = +0,003 \pm 0,025.$$

These values are already corrected for the finite aperture angles of the detectors.

Despite the large error, this value cannot be made to agree with the theoretical coefficients for A_2 and A_4 (p.32). An attempt to explain this discrepancy will be made in another report of our research group (Ref.21).

5. Lifetime and Attenuation of the 1174-Kev Level

From the first two measurements, the lifetime and the attenuation parameter λ_2 can be determined. For defining the lifetime, matching of the eight measured curves for $a_0(\tau_j)$ was done by means of the above-described program. The eight values for the lifetime, calculated from this, were weighted and averaged, yielding the following final value:

$$T_{1/2} = (8.34 \pm 0.20) \text{ nsec.}$$

This value, within the error limits, agrees with a measurement by Herskind and Fossan (Ref.22) who obtained a value of

$$T_{1/2} = (8.7 \pm 0.4) \text{ nsec}$$

for the lifetime.

The matching to the coefficients $A_2(\tau_j)$, required for calculating the $A_2(0)$ values, furnishes eight values for the attenuation parameter λ_2, which are shown in Fig.15. The weighted mean yields the following value for λ_2:

$$\lambda_2 = (0.025 \pm 0.010) \text{ nsec}^{-1}.$$

This large error can be explained by the deficient statistics of the individual measurements. /53

6. Critical Evaluation of the Measurement

To double the measuring time, a simultaneous performance of measurements 1 and 2 could have been done with the described instrument.

For this, the two unused single-channel discriminators of the detectors 3 and 4 could have been connected behind the detectors 1 and 2, whose windows would then have had to be adjusted to the Compton background. In this manner, all eight coincidence circuits would have been used and the subgroups of the multichannel analyzer would have to be reduced to 128 channels; however, this would have changed nothing since, in the interpretation of the described measurements, the contents of several channels were combined for improving the statistics.

This type of measurement could not be performed since the programs for the computer had not been fully worked out at that time so that, with such an arrangement of the single-channel discriminators, no data processing could have been done.

VI. SUMMARY /54

In this paper, formulas for the interpretation of differentially measured

angular correlations were introduced and discussed. The time resolution properties of an instrument, suitable for differential and integral measurements, were used as basis.

This apparatus had been built in collaboration with K.Krien and was described in Chapter II. In contrast to earlier arrangements (Ref.2, 12, 14, 16, 17), this unit had four detectors, which reduces the statistical error of the test data by a factor of 2. The operation of these detectors is controlled by a fully transistorized automatic control unit, which is described in detail.

The data processing of the four-detector unit is done in three steps, using an IBM 7090 computer for which programs were prepared. The computations required for matching with the test data are discussed, and the resultant program is described at length.

Finally, a differential measurement on ytterbium-172 is discussed, for which the described equipment, the derived formulas, and the computer programs were used. With this measurement, the angular correlation coefficients A_2 and A_4 of the 203 - 1095 Kev cascade were to be determined, for which a differential measurement is especially suitable since it permits an elimination of perturbing prompt cascades.

Earlier measurements on this cascade (Ref.17, 19) have shown that the test data strongly contradict the theoretical predictions, so that this measurement was of great interest. The two values

$$A_2 = -0.065 \pm 0.021 \quad \text{and} \quad A_4 = +0.003 \pm 0.025$$

were determined, whose excessive error was produced by the strong Compton background. This value also was impossible to reconcile with the theoretical predictions, so that a discrepancy remains which will be the subject matter of another report of our research group (Ref.21).

In addition, the lifetime of the 1174-Kev level was measured, whose mag- /55
nitude of

$$T_{1/2} = (8.34 \pm 0.20) \text{ nsec}$$

agrees with the value determined by Herskind and Fossan of

$$T_{1/2} = (8.7 \pm 0.4) \text{ nsec}$$

within the error limits.

Measurement of the attenuation factor λ_2 yielded a value of

$$\lambda_2 = (0.025 \pm 0.010) \text{ nsec}^{-1} ,$$

whose large error is due to the statistical indeterminacy of the measurement.

REFERENCES

1. Biederharn, L.C. and Rose, M.E.: Rev. Mod. Phys., Vol.25, p.729, 1953.
2. Forker, M.: Thesis. Bonn, 1965.
3. Special Tubes (Spezialröhren). Valvo Handbook, 1963.
4. Bell, R.E., Petch, H.E.: Phys. Rev., Vol.76, p.1409, 1949.
5. Bell, R.E., Graham, R.L., and Petch, H.E.: Can. J. Phys., Vol.30, p.35, 1952.
6. Simms, P.C.: Rev. Sc. Instr., Vol.32, p.8, 1961.
7. Hrynkiewicz, A.Z.: Nucl. Instr. Methods, Vol.16, p.317, 1962.
8. Matthias, E., Boström, L., Maciel, A., Salomon, M., and Lindtquist, T.: Nucl. Phys., Vol.40, p.656, 1963.
9. Körner, H.J.: Dissertation. Hamburg, 1963.
10. Günther, C.: Dissertation. Bonn, 1964.
11. Abragam, A. and Pound, R.V.: Phys. Rev., Vol.92, p.943, 1953.
12. Lieder, R.M.: Thesis. Bonn, 1964.
13. Krien, K.: Thesis. Bonn, 1966.
14. Radeloff, J.O.: Thesis. Hamburg, 1962.
15. van Soiver, W.J.: IRE Trans. Nucl. Sci., NS-3, No.4, p.39, 1956.
16. Wehmann, U.: Thesis. Bonn, 1965.
17. Voss, J.: Thesis. Bonn, 1965.
18. Gerdau, E.: Thesis. Hamburg, 1960.
19. Günther, C., Blumberg, H., Engels, W., Strube, G., Voss, J., Lieder, R.M., Luig, H., and Bodenstedt, E.: Nucl. Phys., Vol.61, p.65, 1965.
20. Rothenburger, W.: Thesis. Bonn, 1966.
21. Blumberg, H.: Dissertation. Bonn, 1966.
22. Herskind, B. and Fossan, D.B.: Nucl. Phys., Vol.40, p.489, 1963.
23. Harmatz, B., Handley, T.H., and Mihelich, J.W.: Phys. Rev., Vol.123, p.1758, 1961.

Translated for the National Aeronautics and Space Administration by the O.W. Leibiger Research Laboratories, Inc.